

博士論文（要約）

**Effects of surfactant flushing on micromorphology, colloidal and  
hydraulic properties of polluted soils**

（界面活性剤による浄化が汚染土の微細構造やコロイド特性、  
水理学的性質に与える影響）

**Zhuo GUAN**

関 卓

## Abstract

Diesel is commonly used for agricultural machinery and transportation vehicles. Soil contamination with diesel, which is known as a typical light non-aqueous phase liquid in soil, may occur as a result of accidental spillage and leakage and inappropriate use of diesel.

Soil flushing using surfactants has been recognized as a promising in-situ technique for remediation of soil contaminated with low-solubility organic contaminants. During the surfactant-enhanced soil flushing treatment, various interactions between the soil and surfactant solution may take place and lead to changes in soil hydraulic properties and other potential environmental consequences. In-depth understanding of the impact of soil flushing treatment with surfactants on soil properties is critically important for optimizing the design of the treatment process. In this study, soil flushing with linear alkylbenzene sulfonates (anionic surfactant), a common remediation technique for soils contaminated by hydrophobic organic chemicals, was conducted for intact columns (12 cm in diameter) of diesel-contaminated farmland purple soil (entisol) widely distributed in the Upper Reaches of Yantze River. Impact of surfactant-enhanced flushing on soil micromorphology, colloidal and hydraulic properties is investigated. Colloid transport during flushing, diesel removal rate and resulting soil macroporosity change by flushing were quantified.

The study of the temporal variation and vertical migration characteristics of  $C_{12}$ - $C_{28}$  n-alkanes which represent the saturated hydrocarbons of diesel in diesel-polluted soils were conducted. As the results, the concentrations of short-chain even n-alkanes ( $C_{12}$ - $C_{16}$ ) in the soil after 1 year aging in the field decreased drastically while the long-chain even n-alkanes ( $C_{18}$ - $C_{28}$ ) decreased slightly and still presented at relatively high concentrations. The major portion of n-alkanes stayed in the surface soil layer (0-12cm) and hardly migrated downwards to greater depths. After two years aging treatment,  $C_{12}$ - $C_{28}$  n-alkanes in the topsoil decreased more than 80% and n-alkanes migrated downward to the underlying soil lead the concentration of alkanes from 17 cm in depth increased significantly.

Undisturbed soil columns (15 cm in diameter, 12 cm in length) taken at the 0-12 cm and 12-24 cm depth were flushed with LAS and the dynamics of the chemical composition and colloidal properties in effluent were determined. For one year treatment diesel polluted soil, the result showed that, n-alkanes ( $C_{12}$ - $C_{28}$ ) discharge was enhanced by LAS flushing, as compared

water flushing. Removal rate of n-alkanes (representing the diesel) varied with the depth of the topsoil in the range of 14-96% while the low n-alkane residues in the subsoil were completely removed by LAS-enhanced flushing. The colloid concentrations in the effluent during LAS flushing were much higher than those during water flushing. LAS molecular could interact with soil particles and thus mobilize colloids that could migrate through macropores in the purple soil. High concentrations of mobilized colloids could have led to pore plugging to some extent in the middle layer of the soil column, resulting in the observed high LAS residue in the middle of the column than in the surface layer. The Micro-CT scan imaging small cores taken from the tested column after flushing experiments can also corroborate this mechanism. Colloid concentration of the outflow during LAS flushing was much higher than that during water flushing and much larger colloids were observed in the outflow during LAS flushing compared to the water flushing. The X-ray micro-computed tomography (CT) analysis of flushed and unflushed soil cores showed that the proportion of fine macropores (equivalent diameter <250  $\mu\text{m}$ ) was reduced significantly by flushing treatment. The increasing of organic matter after flushing treatment was due to the adsorption of surfactants onto the soil surface, but there was no significant effect on soil contact angle. Soil particle size tended to decrease the proportion of clay by the interaction of the surfactant and soil particles during flushing treatment.

For two year treatment diesel polluted soil, the removal rate of n-alkanes varied with the depth of the topsoil in the range of 1.34-94.28% by LAS-enhanced flushing. It is more difficult for remove n-alkane from soil in the long time aged soil with surfactant. For the no tillage treatment contaminated soil, colloids transport led to pore plugging to some extent in the surface layer of the soil column, which attributed to soil porosity decreased for years. The Micro-CT scan imaging small cores taken from the tested column after flushing experiments for two year treatment diesel polluted soil also showed that the proportion of fine macropores (equivalent diameter <250  $\mu\text{m}$ ) was reduced by flushing treatment.

This phenomenon can be attributed to enhanced clogging of fine macropores by colloids which exhibited higher concentration due to better dispersion by LAS. It can be inferred from this study that the application of LAS-enhanced flushing technique in the purple soil region should be cautious regarding the possibility of rapid colloid-associated contaminant transport via preferential pathways in the subsurface and the clogging of water-conducting soil pores.

Results of this study will provide an overall evaluation of the environmental effects of surfactant flushing on diesel-contaminated soils in support of optimizing this soil remediation technique.

# Table of Contents

Acknowledgements

Executive Summary

List of tables

List of figures

List of abbreviations

1 Introduction

1.1 Background

1.2 Literature review

1.2.1 Soil contamination by diesel and environmental consequences

1.2.2 Principle and application of surfactant-enhanced flushing technique

1.2.3 Effect of surfactant-enhanced flushing on soil chemical properties

1.2.4 Effects of surfactant-enhanced flushing on soil physical and hydraulic properties

1.2.5 Application of X-ray micro-computed tomography for characterization of soil pore structure

1.3 Objectives

1.4 Structure of thesis

2 Desorption characteristics of alkanes from soil with LAS

2.1 Background

2.2 Materials and Methods

2.2.1 Preparation of undisturbed soil box and monitoring of field diesel migration

2.2.2 Batch experiments of diesel desorption from soil with LAS

2.3 Results and Discussion

2.3.1 Temporal changes in alkanes' depth redistributions in soil

2.3.2 Desorption characteristics of alkanes from soil with LAS

2.4 Conclusions

3 Effects of LAS-enhanced flushing on soil chemical properties and the leachate from soil column freshly spiked with diesel

3.1 Background

- 3.2 Materials and Methods
  - 3.2.1 Preparation of repacked soil columns
  - 3.2.2 Diesel spiking and soil column flushing with LAS
  - 3.2.3 Analysis of column outflow and flushed soil
- 3.3 Results and Discussion
  - 3.3.1 Dynamics of LAS and alkanes in column outflow
  - 3.3.2 Removal of alkanes from soil and depth distributions of alkanes and LAS residues in soil
- 3.4 Conclusions
- 4 Effects of LAS-enhanced flushing on packed soil columns
  - 4.1 Background
  - 4.2 Materials and Methods
    - 4.2.1 Preparation of repacked columns with diesel-polluted soil
    - 4.2.2 Soil flushing with LAS and analysis of column outflow
  - 4.3 Results and Discussion
    - Particle size distribution in column outflow
  - 4.4 Conclusions
- 5 Effects of LAS-enhanced flushing on transport of colloids and solutes and various soil properties of diesel-polluted soil after one-year ageing Background
  - 5.1 Materials and Methods
    - 5.2.1 LAS-enhanced flushing experiment through columns of field aged diesel-polluted soil
    - 5.2.2 Analysis of column outflow and flushed soil
  - 5.2 Results and Discussion
    - 5.3.1 Dynamics of EC, LAS, alkanes and particle size distribution in column outflow
    - 5.3.2 Effects on soil hydraulic properties
    - 5.3.3 Effects on soil macroporosity
  - 5.3 Effects on other soil properties Conclusions
- 6 Effects of LAS-enhanced flushing on transport of colloids and solutes and various soil properties of diesel-contaminated soil after two-year field ageing

## 6.1 Background

## 6.2 Materials and Methods

6.2.1 LAS-enhanced flushing experiment through columns of field aged diesel-polluted soil

6.2.2 Analysis of column outflow and flushed soil

## 6.3 Results and Discussion

6.3.1 Dynamics of alkanes, LAS and DOM in column outflow

6.3.2 Effects on depth distributions of LAS and alkanes residues in soil

6.3.3 Effects on soil macroporosity

## 6.4 Conclusions

## 7 Conclusions

7.1 Conclusions

7.2 Future prospective

## References

## **Acknowledgements**

I am very grateful for these wonderful and special years. There are so many people who have helped me go through the whole journey to my RONPAKU program. I would like to acknowledge all the individuals for their great support and understanding.

Firstly, I want to address my sincere appreciation to my Ph.D. home advisor, professor Tang. I am deeply indebted to him for his help and patient guidance throughout the research process. He not only give me the helpful guidance and advice but also the great support for the whole research study in our institute. As a respected mentor of our research team, professor Tang also gave us the thoughtful inputs and constructive comments for our professional development.

Secondly, I would like to express my heartfelt thanks to my Japanese advisor professor Nishimura. Thanks very much for giving me the opportunity to come to the University of Tokyo. He is a respected professor and he give me the guidance and help duiring the whole journey of my PhD study. Thank you for all the thoughtful arrangement, great support and valuable guidance during my study in Japan. He also introduced excellent professors to me to get more useful advice and guidance.

Professor Kato is another respected professor with a great personality. I enjoyed the time learn the experiment from him. I want to express my heartfelt gratitude to him for valuable suggestions and kind encouragements.

Also, I want to thank all the other members, Dr Linlin, Mr. Imoto, Dr Hamamoto, Dr Yamazaki Dr Ishibashi and Dr. Thuyet for their help during my research study in Janpan.

Much appreciation is expressed to my dearest friends, Maomao and Qiuqiu. Thanks for the support during my hard times. They made my research and life times much happier, my tough times much easier. They are not only my friends, they are like family to me.

Thanks are also given to Dr. Chen Liu, Dr. Junfang Chui Dr. Honglan Wang, Huiyun Liu and Jing Qing for their assistance and help in our lab. I enjoyed the time working with them. Also, I would like to express my appreciation to all the other staff and students in my institute. They made my working time more valuable and happy.

At last, I want to thank my family, my mother, father, mother-in-law and father-in-law for theie great support of taking care of my daughter during my research time. I'm so sorry for

having not so much time remain with them. I particularly appreciate my husband in my everyday life for his love and encouragement and great support. I am very lucky to be able to live with him and become more happier and patient than before. During that research time, I have a special gift in my life, a lovely daughter. Thanks for her coming and that her birthing was most important moment for me. I quickly grow up to a responsible mother and became more understanding of my parents infinite love. I love my family very much, I bless them happy and healthy and I have been always wanted them to be proud of me.

### **Executive Summary**

In this study, soil flushing with linear alkylbenzene sulfonate (LAS), a widely used anionic surfactant, is conducted in diesel-spiked soil columns which are collected from the purple soil region in the Upper Reaches of Yangtze River. Impact of surfactant-enhanced flushing on soil micromorphology, colloidal and hydraulic properties, using diesel contaminated columns of different aging time under saturated moisture conditions, were investigated by a combined use of a variety of experimental devices and instruments including gas chromatography, high performance liquid chromatography, Micro computed tomography. The changes in chemical composition of effluents of column experiments, physico-chemical properties of soils (e.g., soil pore structure, water retention characteristics and colloid mobility) are examined. ....

Revelation of surfactant flushing-induced changes in soil micromorphology and colloidal properties.....

Overall evaluation of the environmental impacts of surfactant-enhanced soil flushing treatment.

## **List of tables**

**Table 2-1** Physical and chemical properties of the studied farmland purple soil

**Table 2-2** The proportion of n - alkanes in No. 0 diesel

**Table 2-3** Vertical distribution of n-alkanes in aged soil box for one and two years aging treatment in the field

**Table 2-4** SWRC parameters obtained using Van Genuchten model for initial diesel contaminated soil

**Table 3-1** The n-alkanes residue for topsoil column with freshly added diesel after soil flushing experiments

**Table 5-1** SWRC parameters obtained using Van Genuchten and Bi-exponential model

## **List of figures**

**Figure 1-1.** Schematic of surfactant enhanced-remediation of contaminated soils

**Figure 1-2** In-situ surfactant enhance flushing for soil remediation

**Figure 1-3** Research framework

**Figure 2-1** Yanting Agro-Ecological Experimental Station of Purple Soil

**Figure 2-2** Collection of the undisturbed soil box from an upland cropland field

**Figure 2-3** Experimental scheme of the study.

**Figure 2-4** Stability of n-alkanes in diesel contaminated soil (a) 10g/kg diesel polluted soil Fig. 1(b) 50g/kg diesel polluted soil

**Figure 2-5** Vertical distribution of 9 n-alkanes in aged soil box for one year aging treatment in the field

**Figure 2-6** Vertical distribution of 9 n-alkanes in aged soil box for two year aging treatment in the field

**Figure 2-7** Desorption characteristic n-alkanes by different concentration of surfactants in batch desorption experiment

**Figure 2-8** Soil water retention curves-VG of initial diesel contaminated soil

**Figure 3-1** Experimental scheme of the study

**Figure 3-2** Breakthrough curves for topsoil column with freshly added diesel of 9 n-alkanes in the soil flushing experiments

**Figure 3-3** Breakthrough curves for topsoil column with freshly added diesel of LAS(C<sub>10</sub>-C<sub>13</sub> homologues) in the soil flushing experiments.

**Figure 3-4.** Breakthrough curves for topsoil column with freshly added diesel of colloid, Br<sup>-</sup>, LAS, n-alkanes and EC in the soil flushing experiments.

**Figure 3-5** Depth distributions of LAS residues (C<sub>10</sub>-C<sub>13</sub> homologues) in topsoil column with freshly added diesel columns after LAS-enhanced flushing

**Figure 4-1** Experimental scheme of the study

**Figure 4-2** Chemical properties of outflow samples for packed column in representative collected at different flushing phases. (a) Topsoil packed column with water flushing (b) Topsoil packed column with LAS flushing

**Figure 4-3** Chemical properties of outflow samples for packed column in representative collected at different flushing phases. (a) Subsoil packed column with water flushing (b) Subsoil packed column with LAS flushing

**Figure 4-4** Particle size distributions of colloids in representative outflow samples collected at different flushing phases. (a) Topsoil packed column with water flushing or LAS flushing (b) Subsoil packed column with water flushing or LAS flushing

#### **List of abbreviations**

USTs    Underground Storage Tanks

CMC    Critical Micelle Concentration

LAS    Linear Alkylbenzene Sulfonates

n-alkanes    Normal Alkanes

CT    Computed Tomography

OM    Organic Matter

SWRC Soil Water Retention Curve

HPLC High Performance Liquid Chromatography

GC Gas Chromatography

PARAFAC    Parallel Factor Analysis

## **1 Introduction**

### **1.1 Background**

Soil contamination is a global concern these years. Soil contamination by petroleum products such as diesel, represents a serious environmental problem such as toxicity to animal, plant species and human via food chains and other pathways and being ruins the balance of the ecosystem (Arias-Estévez et al., 2008, Zhang et al., 2002).....

### **1.2 Literature review**

#### **1.2.1 Soil contamination by diesel and environmental consequences**

Soil contamination represents an environmental issue which has become extremely attention due to the diffusion of industrial activities. Petroleum hydrocarbons contamination which become one of the most prominent environmental problems in the present and the future(Ettore Trulli et al.,2016). The continuous production, and utilization of petroleum products to meet the energy needs of the population is usually associated with some environmental pollution problems especially on the soil (Amechi S. Nwankwegua.et al., 2016).

Diesel is a distilled product of petroleum crude, which is widely used fuel for agricultural and industrial machinery, transportation vehicles.It is accounts for over 20% of the total petroleum products and present in the energetic matrix of the majority of countries as an important fuel. Diesel as a kind of petroleum are very complex mixtures consisting of a large number of chemical components belonging to several hydrocarbon groups. The major hydrocarbon groups are saturated hydrocarbons including normal-alkanes (n-alkanes) and naphtenes and other ingredients include isoalkanes, alkenes, cycloalkanes, monoaromatics, polycyclic aromatic hydrocarbons (PAHs) and heterocyclic compounds (Salanitro, 2001).

Soil contamination by diesel, which is known as a typical light non-aqueous phase liquid (NAPL) in soil was widely reported as a result of accidental spillage and leakage and inappropriate use (Hernández-Espriú et al. 2013; Pasha et al. 2012). In China, nearly 70 million tons petroleum went into the environment about 10 million tons petroleum into the soil each year. The national oil pollution of soil area reached about 500 million hm<sup>2</sup>. As a basic fuel, petroleum products of diesel pollution in the soil also reached 30 million hm<sup>2</sup>. Soil contamination with diesel takes place with three ways. Firstly, when the diesel fuel leaks from

underground storage tanks (USTs) during transporting by accidents lead soil and groundwater contaminate (Dineen, 1991). Secondly, For the larger size transport vehicles and agricultural equipment fuel, accidental leakage and illegal dumping lead soil and surfacewater contaminate; Thirdly, the illegal discharge of industrial used as solvents lead soil and water contaminate.

Diesel presence in soil and subsequent leaching to groundwater by leaking and dumping to environment pose a serious threat to aqueous bodies of water, soil ecosystems, and human beings. It will ruin the balance of the ecosystem and cause various environmental and human health damages (Falciglia et al. 2011; Lee et al. 2012). When released in the subsurface, diesel form NAPL like other organic compounds and represent a long-term source of groundwater contamination for the reasons that maximum concentration limits of the contaminations are much lower than the effective solubility of most NAPL component. (Leticia A. Bernardez et al. 2009)

#### 1.2.2 Principle and application of surfactant-enhanced flushing technique

Due to the great harm for human health caused by soil contamination, there was great efforts to develop environmentally sound and cost-effective techniques for remediation of a variety of contaminated soils. Many remedial attempts such as surfactant flushing, chemical oxidation, phot catalysis remediation, biodegradation to clean up sites contaminated by chemical, physical or biological effects have been made to achieve an environmentally sound and cost-effective remediation of contaminated lands (Lohi et al., 2008). Impractical remediation for contaminations with low water solubility, soil washing is a mechanical process that uses aqueous solutions with surfactants to remove chemical pollutants from soils. Basic concepts and description of the in situ soil flushing technique are provided by US EPA (2006) and Lee et al. (2007). In situ soil flushing using surfactants (surfactant-enhanced flushing) has been recognized as a promising time-efficient and versatile remediation technology for remediation of soils contaminated by low-solubility organic chemicals (Cowell et al. 2000; Mao et al. 2015; Trelu et al. 2015) and therefore attracts increasing attentions in recent years (Svab et al. 2009; Davezza et al. 2011; Rosas et al. 2011).

Surfactants are a group of amphiphilic chemicals which contain both hydrophilic and hydrophobic parts in the molecular structure (Vishnyakov et al. 2013). Surfactants' unique molecular structures allow enhancing the water solubility and mobilization of soil contaminants

(Dwarakanath et al. 1999) for reduce the free energy of the system, especially for hydrophobic organic compounds (Lee et al. 2013). Variety of surfactants, e.g., ionic and nonionic surfactants, gemini surfactants, biosurfactants and mixed surfactant systems were applied to soil remediation (Fountain et al., 1996). Some kind of surfactant can enhance desorption of pollutants from soil, and promote bioremediation of organics by increasing bioavailability of pollutants (Lestan et al., 2008). Surfactant molecules are introduced into a water-soil contaminated system, the mechanism of surfactant enhanced-remediation of contaminated soils shown in Fig. 2. There are two different mechanism with different concentration of surfactant: soil roll-up mechanism and solubilization with the concentration of surfactant occurs below or above critical micelle concentration (CMC) ( Dermont et al., 2008; Lee et al. 2007; Mulligan et al. 2001). Normally, lipophilic part of the surfactant tend to combine with hydrophobic contaminants or soil particles, the hydrophilic part are more easily enter into aqueous phase. Surfactant monomers with lower concentration (below CMC) tend to be combine the interfaces of the soil and contaminate and change the wettability of the system by increasing the contact angle between the soil and the hydrophobic contaminants. The surfactant molecules will form micelles with the increasing of surfactant concentration, micelles begin to form is termed the critical micelle concentration. With increasing concentrations, surfactant molecules gradually replace the interfacial water to lower polarity of the aqueous-phase and decreased surface tension and accelerated dissolution of the contaminants. At the same time, surfactant enhance the solubilization of hydrophobic organic pollutants in the micelles solubility. With further increasing concentrations (above CMC), surfactant molecules will form spheroid and lamellar structures gradually like micelles and lower polarity of the aqueous-phase and decreased surface and interiors tensions ( Bettahar et al. 1999 ; Sabatini et al. 1999 ). The partition of pollutants in the aqueous phase thereby remarkably increases [16]. For surfactant enhance soil washing process, the dissolved contaminates in the surfactant micellar phase was pump to the surface of the polluted sites for further separation [17] and treatment or used as the recycle washing solutions. Part of the contaminated still remain in the soil for plant uptake and microbial degradation. The schematic of in-situ surfactant-enhanced flushing as shown in Fig. 1 . Surfactants solution are injected into the area of contamination via injection wells. The soil contaminants such as (NAPL) contaminant are mobilized by solubilization or chemical

interactions. After passing through the contamination zone, the eluent contain surfactants and eluted contaminants is collected for further pollution treatment and reinjection (Mulligan et al. 2001).

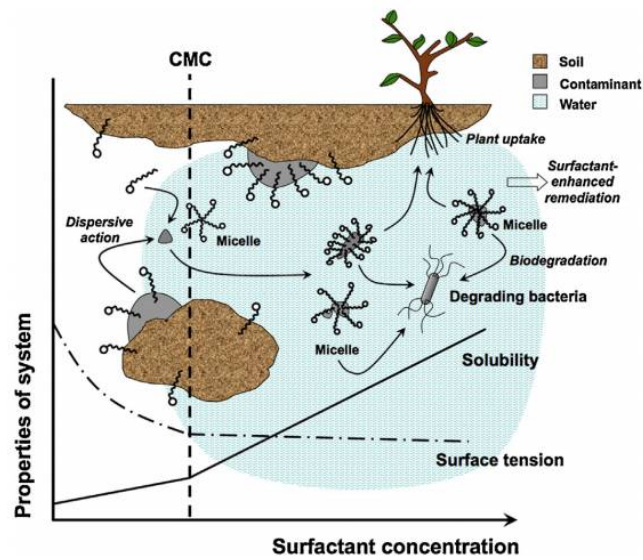


**Figure 1-1.** Schematic of surfactant enhanced-remediation of contaminated soils .(Mao et al, 2015)

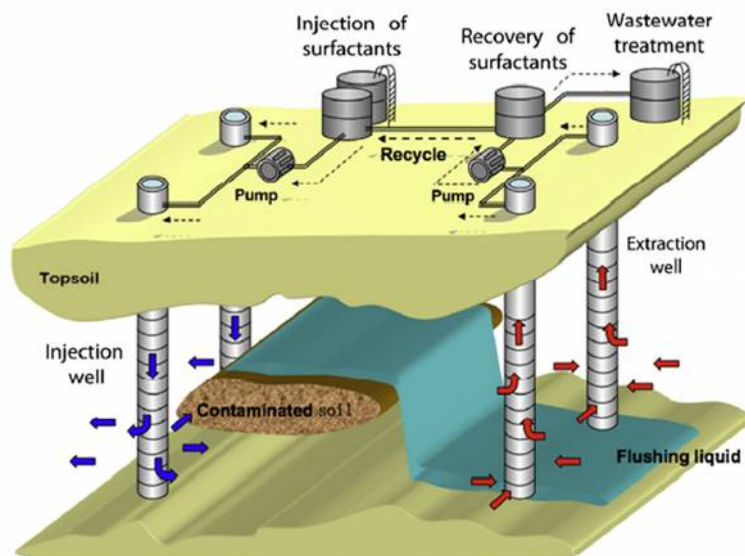


**Figure 1-2** In-situ surfactant enhance flushing for soil remediation (Mao et al, 2015)

The schematic of in-situ surfactant-enhanced flushing as shown in Fig. 1 . Surfactants solution are injected into the area of contamination via injection wells. The soil contaminants such as (NAPL) contaminant are mobilized by solubilization or chemical interactions. After

passing through the contamination zone, the eluent contain surfactants and eluted contaminants is collected for further pollution treatment and reinjection.

### 1.2.3 Effect of surfactant-enhanced flushing on soil chemical properties

The applications of surfactants-enhanced flushing technique for contaminated soils have been extensively investigated (Lee et al. 2015; Khalladi et al. 2009; Lee et al. 2013; Park and Bielefeldt 2005) focusing mostly on the selection of surfactants showing high removal efficiency, low cost and toxicity on soil microorganisms (Hernández-Espriú et al. 2013).

To enhance the removal efficiency, a combination of processes may be applied to contaminated sites because each process has some technical restrictions when applied to actual contaminated sites (Lee et al. 2011).

An elimination rate of 97% was achieved after a soil washing by 8 mM SDS solution with a rate 3.2 mL/min. Water washing of a diesel-polluted soil could eliminate up to 24% of nalkanes. (Razika Khalladi et al.2009). Chang et al. found that, 73.6 up to 100% of polycyclic aromatic hydrocarbons (PAHs) were eliminated in the presence of sodium dodecyl sulfate (SDS), while 30–80% when using only water (Chang et al., 2000 )Liu et al. ()showed that the increase in the apparent solubility of some PAHs in the presence of anionic and non-ionic surfactants increases significantly beyond the CMC. Regarding the surfactant soil washing experiments, ionic surfactants showed removal rates above the control test of about 78.51 % (Maranil LAB), 71.27 % (Texapon 40), 60.13 %(SDS), and 48.19 % (Surfacpol G). In contrast, some nonionic surfactants showed removal rates below soil-washin background rate (40 %). On the other hand, natural gums showed interesting and promising results.(Antonio Hernández-Espriú et al. 2013)

An ex situ soil column washing experiment was performed on a genuinely diesel-contaminated soil. The washing solution was enriched with surfactant Tween 80 at different concentrations, higher than the critical micellar concentration (CMC). The impact of soil washing was evaluated on the hydrocarbons concentration in the leachates collected at the bottom of the soil columns. These eluates were then studied for their degradation potential by EF treatment. Results showed that a concentration of 5% of Tween 80 was required to enhance hydrocarbons extraction from the soil. Even with this Tween concentration, the efficiency of the treatment remained very low (only 1% after 24 h of washing).

#### 1.2.4 Effects of surfactant-enhanced flushing on soil physical and hydraulic properties

The surfactant-enhanced soil flushing treatment involves various interactions between the soil and surfactant solution which may cause changes in soil hydraulic properties along with other potential effects. (Renshaw et al. 1997; Jia et al. 2005; Laha et al. 2009). The mechanisms responsible for the change in hydraulic conductivity may include changes in fluid characteristics (e.g., the reduction of fluid surface tension, the formation of micelles), the destruction of soil aggregate structure and resultant release of fine particles, clay swelling, fine clay particle mobilization, precipitation of surfactants with cations (e.g.,  $\text{Ca}^{2+}$ ,  $\text{Mg}^{2+}$ ), mineral dissolution and precipitation (e.g., Liu and Roy, 1995; Tumeo, 1997). For example, hydraulic conductivity reduction was observed in the loamy soils (Gabr et al. 2011); immediate plugging of soil columns followed surfactant injection (Roy et al. 1995). Contrastingly, some other researches have shown that, extensive soil column tests achieved high oil recoveries exceeding 99% without significant problems such as pore clogging and high surfactant retention (Dwarakanath and Pope 2000).

#### 1.2.5 Application of X-ray micro-computed tomography for characterization of soil pore structure

The visualization and quantification of macropores are essential for a better understanding of soil structure. X-ray micro-computed tomography (Micro-CT) imaging is a non-destructive technique for characterise the pore space to characterise cross-sectional and three-dimensional internal structures (Lindquist et al., 1996; Schlüter et al., 2014) by constructing synthetic 3D images from high resolution 2D thin sections using statistical methods. In recent years, Micro-CT scanning has been employed to study the characteristics of soil macropores to visualize and quantify the characteristics (e.g. number, size and location) of soil macroporosity (Lamande et al. 2013; Wang et al. 2016).

Specific details of these imaging techniques and their evolution can be found in previous reviews (Blunt et al., 2013; Ketcham and Carlson, 2001).

To image geological porous materials at the micro-scale, three types of micro-CT systems are in common use: medical CT, industrial X-ray generation tube and synchrotron micro-tomography. They primarily differ in X-ray energy and source, means of sample manipulation

and detector geometry. Although the best image resolution reported in the literature is from synchrotron micro-CT, the samples need to be relatively small to achieve these resolutions. This may result in poor statistical representation of the bulk material. Typical spatial resolution that medical CT systems can achieve is between 200 and 500  $\mu\text{m}$ , industrial systems range from 50 to 100  $\mu\text{m}$  and synchrotron based CT systems can reach from 1  $\mu\text{m}$  to 50  $\mu\text{m}$  (Wildenschild et al., 2002a). Presently, laboratory systems with genuine submicron capabilities exist, some with voxel resolution of 20 nm, providing spatial resolution of 50-60 nm. Three main configurations are used in systems that seek submicron resolution; a good review can be found in (Schlüter et al., 2014; Withers, 2007).

### **1.3 Objectives**

The objective of this study is to gain new insights into adverse impacts of LAS-enhanced flushing for purple soil, using undisturbed columns of diesel-contaminated farmland soil aged in the field for different times with special regards to colloid transport and soil macroporosity. The results of this study could also be supportive to full evaluation of the feasibility of this soil remediation technique for field application in not only this studied entisol but also other poorly structured, aggregated soils.

## 1.4 Structure of thesis

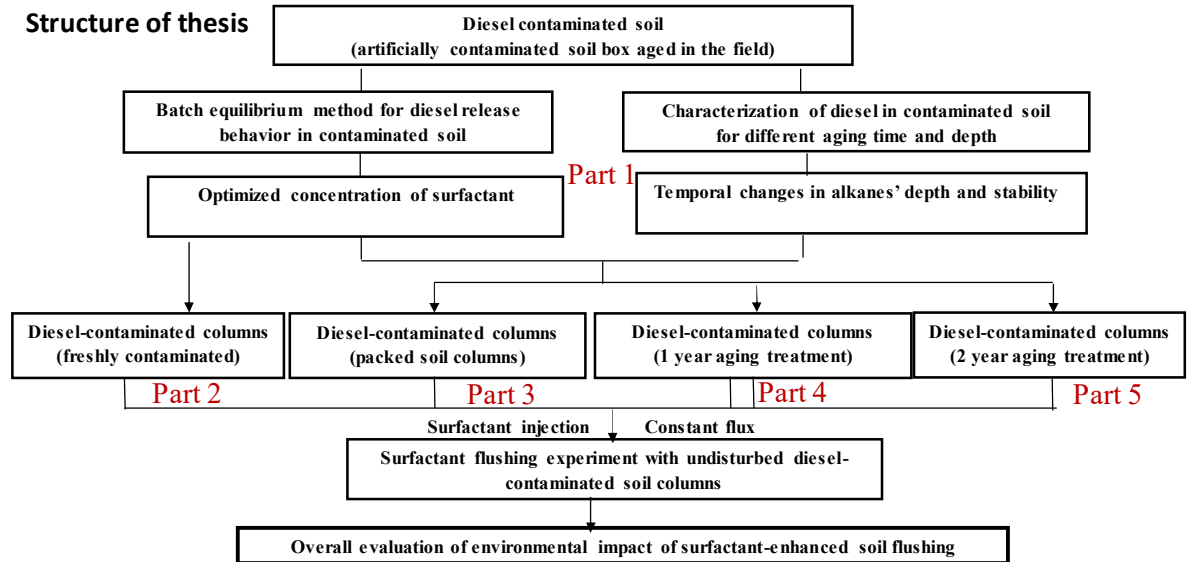


Figure 1-3 Research framework

## **2 Desorption characteristics of alkanes from soil with LAS**

### **2.1 Background**

Diesel fuel occupies more than 20% of the total petroleum Products ( Do-Yun Yu et al. 2007) Diesel fuel is a multi- component contaminant including various molecular weight alkanes. A commercially available diesel fuel usually includes up to 80% alkanes and these alkanes are comprised of 50% normal alkanes and 50% iso- or cycloalkanes (Lee et al., 1992) Diesel fuel is composed of 60% of saturated hydrocarbons ( n-alkanes and naphtenes) and 40% of aromatics (Razika Khalladi et al. 2009)

The applications of surfactants-enhanced flushing technique for contaminated soils have been extensively investigated (Lee et al. 2015; Khalladi et al. 2009; Lee et al. 2013; Park and Bielefeldt 2005) focusing mostly on the selection of surfactants showing high removal efficiency, low cost and toxicity on soil microorganisms (Hernández-Espriú et al. 2013). Among other surfactants, linear alkylbenzene sulfonates (LAS) as widely used anionic surfactant (Guan et al. 2008) are of great interest for soil remediation companies. Although this technique is generally efficient to clean up soil, the major concern remains because of mixed results of its application in soil matrix (Urum et al. 2006).

Ionic surfactants include cationic, anionic, and zwitterionic surfactants. Most soil colloidal particles are negatively charged, and they can bind with cationic and anionic surfactants by ion exchange and ion matching. The consequent decrease of the interfacial tension between soil and water facilitates the migration of pollutants. surfactants, cationic surfactants are more likely to adsorb onto the surface of negatively charged soil particles and aquifer materials, which inevitably increased the consumption of surfactants. Other commonly used surfactants include cetyltriethyl ammonium bromide (CTAB), sodium dodecyl benzene sulfonate (SDBS), and cocamidopropyl betaine. In comparison with anionic Therefore, more cases that use anionic surfactants, instead of cationic surfactants, for soil washing or aquifer flushing were reported.

In our study to characterize surfactant desorption diesel release behavior in contaminated purple soils, the optimize the surfactant concentration to achieve high removal efficiency of diesel were executed ..

### **2.2 Materials and Methods**

### 2.2.1 Preparation of undisturbed soil box and monitoring of field diesel migration

A large intact soil sample in a box (0.8 m in depth, 2 m in length and 1 m in width) was taken from an agricultural field at Yanting Agro-Ecological Experimental Station of Purple Soil (31°16' N, 105°27' E) (Figure 2.1) located at hilly central Sichuan, SW China. The sampling box was made of stainless iron and a layer of gravel (10 cm in thickness) was placed under the soil to allow free drainage through the outlet holes at the bottom of the box, the collection of the soil box was showed in figure 2.2. The field was cultivated in wheat-maize rotation and, according to profile inspection and the interview with farmers, the depth of plow layer was 10-15 cm at the time of sampling, which had been shallower than before (about 25 cm) since early 2000s. The soil (classified as an entisol according to the soil taxonomy of the United States Department of Agriculture) has, on average, a pH of 8.5 and 13.72 g kg<sup>-1</sup> organic matter content, and contains 28% sand, 40% silt and 32% clay (Table 1). The main minerals of the soil are quartz, plagioclase, K-feldspar, calcite, smectite and illite.



**Figure 2-1** Yanting Agro-Ecological Experimental Station of Purple Soil

Undisturbed soil core samples (100 cm<sup>3</sup>) were taken at different soil depths (0-10, 10-20, 20-30, 30-40 and 40-50cm) before and after the plowing treatment of the soil box for measure saturated hydraulic conductivity and soil water retention curve. After 1 week of plowing treatment, 6 kg of No. 0 diesel was artificially spiked onto the surface of the undisturbed soil box. The soil box was placed in the field and subjected to two years of natural drying-wetting cycles without plowing operation. The weeds were removed by hands. Different depths of soil samples were also collected from the box after aging 1 and 2 years for monitoring of field diesel vertical migration behaviors. Scheme of the experimental procedures used in this study is shown in figure 2.3.

**Table 2-1** Physical and chemical properties of the studied farmland purple soil

Sample	Depth (cm)	pH	Organic matter (g kg <sup>-1</sup> )	Soil texture (%)		
				Sand	Silt	Clay
Topsoil	0-12	8.52	13.53	27	40	33
Subsoil	12-24	8.47	13.91	28	41	31



**Figure 2-2** Collection of the undisturbed soil box from an upland cropland field

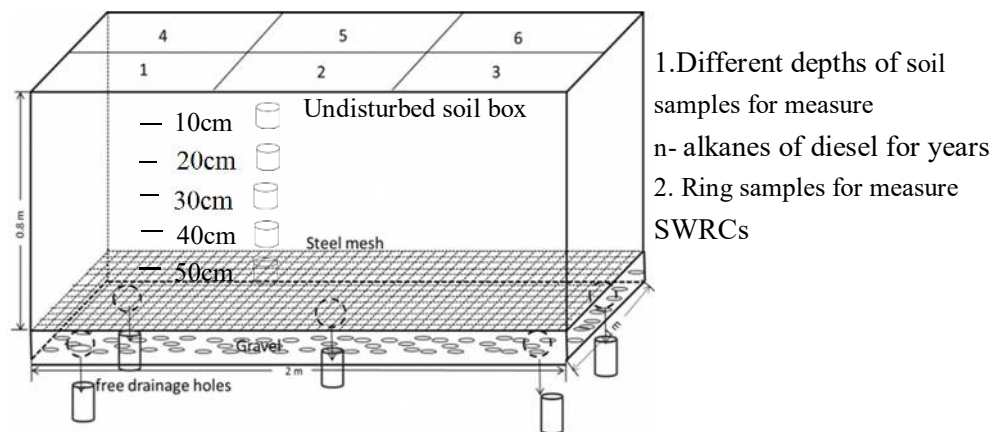


**Figure 2-3** Experimental scheme of the study.

### 2.2.2 Batch experiments of diesel desorption from soil with LAS

#### Materials

An orchard and an upland field at Yanting agro-ecological Experimental Station of Purple soil, Chinese Academy of Sciences, are chosen for this study. Soil samples (at depth of 0-10, 10-20, 20-30, 30-40, 40-50 cm) were collected, and each sample is divided into two subsamples: a fresh subsample and an air-dried and sterilized subsample for comparison study. The soil sample is artificially spiked with diesel and is subject to ageing process for 2 months. The diesel-contaminated soils are used for desorption experiments with linear alkylbenzene sulfonate (LAS) solutions by batch equilibrium method and unsaturated transient flow method.

On the other hand, an undisturbed soil flume (0.5 m in depth, 2 m in length, and 1 m in width) is taken from each field site with a stainless container with free drainage system at the bottom. The soil flume is then transported back to the laboratory, and  $2.6 \times 10^5$  mg-diesel/m<sup>3</sup> is artificially spiked into the soil. Afterwards, artificial rainwater events are performed once a week to mimic natural diesel vertical migration in soil profile. After two months of this treatment, undisturbed soil columns (10 cm in diameter, 10 cm in length) are collected at depth of 0-10, 10-20, 20-30, 30-40, 40-50 cm with stainless steel cylinders in both horizontal and vertical direction. Both the vertically and horizontally collected soil columns are used for soil flushing experiments with LAS solutions and artificially rainwater.

#### Optimization of the surfactant formula and concentration

Diesel (at  $1 \times 10^5$  mg/kg concentration) is added into fresh (moist and unsterilized) soil samples and air-dried and sterilized soil samples, which are subsequently subject to wetting-drying treatment (using artificial rainwater representative of Yanting) for 2 months. The contaminated soil is extracted with alkylbenzene sulfonate solutions whose concentrations are 1, 2.5, 5, 10 and 20 times of the critical micelle concentration (CMC). Batch equilibrium method and unsaturated transient flow method (Katou et al., 2001) are employed to determine the desorption/dissolution (e.g.,  $K_d$ ,  $K_{oc}$ ) of diesel and the sorption of LAS, and to establish the optimal formula and concentration of LAS to be used in subsequent column experiments.

The concentration of diesel and LAS in water samples (filtered through a 0.45  $\mu$ m filter) and soil samples are solvent extracted, purified, concentrated and subsequently analyzed with gas chromatography with a flame ionization detector (GG/FID, 7890A, Agilent, USA) and high performance liquid chromatography (HPLC, 1260, Agilent, USA) with a UV detector, respectively.

Before desorption experiments, main components of diesel and the stability of main components in soil was determined in lab.  $10000 \text{ mg kg}^{-1}$  and  $50000 \text{ mg kg}^{-1}$  No. 0 diesel was artificially spiked onto the soil which was mixed topsoil collected from the soil box before contaminated treatment. The soil was placed in lab and subjected to one month of artificial drying-wetting cycles treatment and seal for half a year for determine the diesel variation characteristics of diesel in purple soil.

The preliminary results showed that the critical micelle concentration (CMC) was 658.43 mg L<sup>-1</sup>. Desorption experiments using a batch equilibrium method at 25 °C at the presence of different concentrations of LAS was conducted for diesel-contaminated soils. 10 mL of 0, 1, 3, 5, 7, 9, 10, 11, 12, 13, 15 CMC initial LAS concentrations in deionized water were added to 30 mL glass jars with Teflon screw caps containing 1 g diesel polluted soil. Desorption samples were agitated in a constant temperature oscillator at a constant speed of 200 rpm for 24 hours. After that, samples centrifuged at 3400 rpm for 10 min and supernatants filtered through 0.45 μm filter for the determination of diesel concentration.

The SPE cartridge was prepared by modifying a SPE column (6 mL, polypropylene), which was purchased from SUPELCO Cooperation, USA. The C18 packing was evacuated and 0.2 g CMMWCNTs were packed in the column. The polypropylene upper frit was reset at the upper end of the column to prevent the CMMWCNTs losses during the operation process. Then the outlet tip of the column was connected to a model SHZ-3(III) vacuum pump (Yuhua Instrument Co. Ltd., Zhengzhou, Henan), and the inlet end of column was connected to PTFE suction tube whose other end was inserted into sample solution. In order to prevent CMMWCNTs leaking, a layer of glass wool was put in the bottom of the cartridge. Using the glass wool in the bottom of the cartridge can also reduce the clogging of the packed CMMWCNTs.

After the packed cartridge was preconditioned by 5 mL methanol and 5 mL ultra pure water, respectively, the appropriate volume of sample solutions spiked with LAS was passed through the cartridge at the flow rate of 4 mL min<sup>-1</sup> by a vacuum pump. (Note that the sample solutions containing LAS was treated ultrasonically before passing through the cartridge. The ultrasonic experiments were performed by placing the 1 L volume flask containing sample solution into an ultra-sonic bath, then the power was turned on for the given time.)

Then rinsed with 10 mL of ultra pure water prior to the elution to remove the co-absorbed matrix materials from the cartridge and dried under a certain negative pressure (20 mmHg) for 10 min. Subsequently, analytes retained on the cartridge were eluted with an optimal volume of methanol. The eluate was evaporated to dryness under a stream of nitrogen at 40 °C and the residue was reconstituted with 0.5 mL ultra pure water, and then used for HPLC-UV analysis for LAS.

The final concentrations of diesel remaining in the aqueous phase were determined using HPLC-UV after SPE enrichment.

Nine even *n*-alkane homologues (C<sub>12</sub>-C<sub>28</sub>) which were chosen to represent the main saturated hydrocarbons constituting the diesel used in this study. Methods for sample pretreatment and analysis were optimized. Soil samples were pretreated by ultrasonic-assisted dispersive solid phase extraction with activated carbon clean-up method prior to analysis for gas chromatography with a flame ionization detector (7890A GC-FID, Agilent, USA), an Agilent autosampler and Agilent 19091J-413 column (30 m×0.32 mm i.d.) with a nominal film thickness of 0.25 μm. The detailed procedure for sample pretreatment was: 2 g of soil sample was extracted by 10 mL of hexane mixed with 5 g of anhydrous sodium sulfate in a ultrasonic device (at 300 W) for 90 min and the extract was filtered through a 0.45-μm polyamide filter membrane after centrifugation, the filtrate was purified with 0.01g of activated carbon and filtered through 0.45 μm. The filtrate was then concentrated to near dryness in a rotary evaporator (BUCHI, Switzerland) and then 1 mL of hexane (Merck KGaA, Germany) was added to dissolve the target compounds for subsequent analysis with the GC-FID. The injector and detector temperatures were set at 250 and 330°C, respectively. N<sub>2</sub> was used as carrier gas at a flow rate of 1 mL min<sup>-1</sup>. The column temperature was programmed as follows: increased from 70°C (held for 2 min) to 300°C at 4°C min<sup>-1</sup> and then held at 300°C for 5 min. 2 μL of the sample was injected manually in the splitless mode. The detection limits were 0.01-0.05 mg L<sup>-1</sup> for C<sub>12</sub>-C<sub>28</sub> *n*-alkanes.

Soil cores taken from different depths were measured for the Single- and Dual-Porosity Soil Water Retention Curves. To obtain the  $\theta(h)$  dataset, soil cores were saturated with water from the bottom and brought successively to equilibrium in a sandbox for the suctions of -1, -2.5, -10, -31.6, -63.1 and -100 cm H<sub>2</sub>O and in pressure chambers (Soil moisture Equipment Corp., Santa Barbara, CA, USA) for the suctions of -337, -510, -1,020, -2,040, 248 -5,100 and -15,300 cm H<sub>2</sub>O (Cornelis et al. 2005). Soil water content was determined by weighing. Finally, the soil cores were oven dried at 105 °C for 24 h and weighed again to determine the final water content and dry bulk density which were calculated on a volumetric basis.

Soil water retention data measured on the soil core samples were fitted to the single-

porosity van Genuchten (1980) model.

The van Genuchten model (1980) can be written as

$$S^*(h) = \frac{\theta(h) - \theta_{r-vG}}{\theta_{s-vG} - \theta_{r-vG}} = \frac{1}{\left(1 + |\alpha_{vG} h|^n\right)^m} \quad [1]$$

$$h_{inf} = \frac{1}{\alpha} \left(\frac{1}{m}\right)^{1/n} \quad [2]$$

$$\theta_{inf} = \theta_{r-vG} + (\theta_{s-vG} - \theta_{r-vG}) \left(1 + \frac{1}{m}\right)^{-m} \quad [3]$$

$$S_{inf} = -n(\theta_s - \theta_{r-vG}) \left(1 + \frac{1}{m}\right)^{-(1+m)} \quad [4]$$

where  $S^*$  is the relative water saturation of the soil,  $h$  is the pressure head (cm),  $\theta_{s-vG}$  and  $\theta_{r-vG}$  are the saturated water content and residual water content, respectively ( $m^3 m^{-3}$ ), and  $\alpha_{vG}(cm^{-1})$ ,  $n$ , and  $m (= 1 - 1/n)$  are empirical parameters;  $n$  is related to the slope of the SWRC at the inflection point (Jirků et al., 2013), which can be used as an indicator of soil physical quality (Dexter, 2004). The van Genuchten (1980) parameters were estimated using the RETC fitting program (van Genuchten et al., 1991). The van Genuchten (1980) SWRC has a unique inflection point where the curvature is zero or where it changes from convex to concave. In this study, curve slope ( $S_{inf}$ ), soil water content ( $q_{inf}$ ), and the pressure head ( $h_{inf}$ ) at the inflection point of the SWRC<sub>vG</sub> were calculated as (Dexter and Czyz, 2007)

Same methodology for the measurement of soil water retention curves (SWRCs) and analysis were carried out for soil cores taken from soil column.

$$\phi = 1 - \frac{\rho_b}{\rho_s} \quad \theta(h) = \theta_r + \frac{\theta_s - \theta_r}{[1 + (\alpha h)^n]^m}$$

Porosity ( $\phi$ ) was calculated as where  $\rho_b$  and  $\rho_s$  are the bulk and particle densities ( $g cm^{-3}$ ), respectively. The water content vs pressure head data were fitted using the function of van Genuchten (1980): where  $\theta$  is the volumetric water content ( $m^3 m^{-3}$ ),  $h$  is pressure head (cm) (taken as a positive value),  $\theta_r$  and  $\theta_s$  are the residual and saturated water contents ( $m^3 m^{-3}$ ), respectively,  $\alpha$  ( $cm^{-1}$ ),  $n$ , and  $m (= 1 - 1/n)$  are empirical parameters.

Soil physical parameters were derived from the SWRCs, including soil matrix porosity ( $\theta_m$ ), macroporosity (MacPor), air capacity (AC) and plant-available water capacity (PAWC).

$\theta_m$  is defined as the volumetric water content retained by soil textural pores (exclusive of macropores), which corresponds to pore diameters of  $\leq 75\mu\text{m}$ . Thus, MacPor refers to pores with diameter  $\geq 75\mu\text{m}$ . AC is an indicator of soil aeration, and PAWC is a parameter indicating the capacity of the soil to store and provide available water to plant roots. These parameters were calculated as follows (Reynolds et al 2007): PAWC is a parameter indicating the capacity of the soil to store and provide available water to plant roots. These parameters were calculated as follows (Reynolds et al 2007):

$$\text{MacPor} = \theta_s - \theta_m$$

$$\text{AC} = \theta_s - \theta_{\text{FC}}$$

$$\text{PAWC} = \theta_{\text{FC}} - \theta_{\text{PWP}}$$

Where  $\theta_m$  was determined at the matric head of  $-40$  cm in this study;  $\theta_{\text{FC}}$  and  $\theta_{\text{PWP}}$  are the volumetric water contents at field capacity ( $h = -340$  cm) and at permanent wilting point (PWP) ( $h = -15,300$  cm), respectively.

Moreover, since each SWRC has a unique inflection point where the shape of SWRC changes from convex to concave, another parameter was defined as the inflection slope ( $S_{\text{inf}}$ ), which can be used as a measure of soil microstructure. A more negative  $S_{\text{inf}}$  indicates a better soil physical quality. It was calculated using the following equation (Dexter 2004):

$$S_{\text{inf}} = -n(\theta_s - \theta_r) \left( \frac{2n-1}{n-1} \right)^{\left( \frac{1}{n}-2 \right)}$$

PSDs were calculated as the derivative of the equivalent  $\theta(r)$  curve converted from the fitted SWRCs, where  $r$  ( $\mu\text{m}$ ) is the maximum equivalent radius of pore that remains full of water at a given pressure head  $h$  (cm). Here,  $r$  can be calculated from  $h$  using the Young-Laplace equation (Vomocil and Flöckner 1965):

$$r = \frac{1490}{|h|}$$

## 2.3 Results and Discussion

### 2.3.1 Temporal changes in alkanes' depth redistributions in soil

**Table 2-2** The proportion of n - alkanes in No. 0 diesel

	C <sub>12</sub>	C <sub>14</sub>	C <sub>16</sub>	C <sub>18</sub>	C <sub>20</sub>	C <sub>22</sub>	C <sub>24</sub>	C <sub>26</sub>	C <sub>28</sub>
mg g <sup>-1</sup>	14.00	15.13	16.94	9.67	10.84	5.83	2.71	0.81	0.18
%	18.39	19.88	22.26	12.70	14.25	7.65	3.57	1.06	0.24

Figure skipped

**Figure 2-4** Stability of n-alkanes in diesel contaminated soil (a) 10g/kg diesel polluted soil Fig. 1(b) 50g/kg diesel polluted soil.

(A and C: aging soil which was subject to 1month of drying-wetting cycle treatment in lab ;

B and D: aging soil which was subject to 6 month of drying-wetting cycle treatment in lab)

Soil samples from different depths in the undisturbed soil flume after one year aging treatment were collected for determine the vertical migration characteristics of even C<sub>12</sub>-C<sub>28</sub> n-alkanes, which represent the saturated hydrocarbons of diesel. The depth distribution of n-alkanes in the undisturbed diesel-polluted soil flume (Table 2) showed that most of n-alkanes stayed in the surface layer (0-12cm), especially C<sub>16</sub> to C<sub>26</sub> n-alkanes, there were much higher residuals in the surface after one year aging in the field. But most of the n-alkanes could hardly migrate downwards to greater depths; there were less than 10 mg/kg contaminants were detected in the subsurface. The reason is that, most of the alkane of diesel belong to light oil and are not easily migrated downwards beside evaporation. Therefor the temporal variation of n-alkanes was also explored to examine the effect of evaporation and biodegradation of diesel on purple soil. By comparing diesel-polluted purple soils that had been aged for 1 month and 6 months in the laboratory, the concentration of short-chain even n-alkanes (C<sub>12</sub>-C<sub>14</sub>) in the soil decreased greatly with time, but the concentration of the long-chain even n-alkanes (C<sub>16</sub>-C<sub>28</sub>) did not change significantly both at the initial diesel addition level of 10 g/kg and 50 g/kg. Similarly, the concentrations of short-chain even n-alkanes (C<sub>12</sub>-C<sub>14</sub>) in the soil after 1 year

aging in the field condition decreased drastically while the long-chain even n-alkanes (C<sub>16</sub>-C<sub>28</sub>) decreased slightly and still presented at relatively high concentrations. These observations suggest that the short chain n-alkanes dissipated from the soils probably via volatilization and biodegradation; the long-chain n-alkanes are more stable and slowly migrate longitudinally, and are less affected by volatilization and biodegradation. Therefore, the diesel contaminants once leaked onto the surface of the soil are still having high residual concentration after one year aging and appropriate soil remediation methods are needed for ecological environment. Temporal variation and vertical migration of n-alkanes Long chain N-alkanes has higher stability and N-alkane may not migrate into deeper soil

Figure skipped

**Figure 2-5** Vertical distribution of 9 n-alkanes in aged soil box for one year aging treatment in the field

**Table 2-3** Vertical distribution of n-alkanes in aged soil box for one and two years aging treatment in the field

Depth(cm)	Aging time (years)	mg kg <sup>-1</sup>								
		C <sub>12</sub>	C <sub>14</sub>	C <sub>16</sub>	C <sub>18</sub>	C <sub>20</sub>	C <sub>22</sub>	C <sub>24</sub>	C <sub>26</sub>	C <sub>28</sub>
0-4	1	0.13±0.05	6.46±0.49	66.03±3.17	226.59±8.75	139.34±8.74	68.00±6.63	30.54±2.44	7.60±0.94	1.37±0.20
	2	--	1.10±0.13	11.08±0.38	44.25±1.79	21.57±2.31	10.85±2.46	6.26±2.44	1.76±0.23	0.28±0.06
5-8	1	0.18±0.00	4.71±1.57	43.61±12.15	159.19±46.01	78.14±27.86	47.09±10.77	21.48±4.32	6.25±0.82	1.02±0.23
	2	--	2.03±0.04	18.39±0.83	70.40±0.67	37.21±0.39	21.76±0.27	9.98±4.32	2.55±0.13	0.32±0.03
9-12	1	0.18±0.03	0.74±0.19	7.35±3.49	40.15±12.19	25.78±9.39	18.57±5.32	9.59±3.24	2.85±1.17	0.44±0.16
	2	--	0.34±0.03	1.86±0.84	11.55±1.21	6.01±2.28	4.31±1.93	2.29±3.24	1.34±0.60	0.38±0.20
13-16	1	0.09±0.02	0.36±0.06	1.47±0.52	4.26±1.96	5.30±2.66	3.95±2.07	2.19±1.05	0.73±0.24	0.43±0.13
	2	--	0.25±0.02	0.57±0.05	3.07±0.65	1.66±0.22	1.12±0.03	0.78±1.05	0.43±0.11	0.09±0.01
17-20	1	0.06±0.03	0.35±0.02	0.45±0.04	0.77±0.11	0.75±0.23	0.65±0.13	0.42±0.08	0.22±0.02	0.65±0.14
	2	--	0.35±0.02	0.93±0.18	1.96±0.09	1.43±0.28	1.01±0.12	0.67±0.08	0.39±0.03	0.10±0.02
21-24	1	0.06±0.03	0.33±0.01	0.52±0.09	0.93±0.06	0.94±0.00	0.72±0.04	0.43±0.02	0.22±0.02	0.49±0.02
	2	--	0.26±0.02	0.75±0.00	2.41±0.34	1.64±0.19	1.19±0.07	0.84±0.02	0.50±0.03	0.14±0.00
25-30	1	0.05±0.02	0.31±0.04	0.44±0.04	0.54±0.03	0.41±0.06	0.37±0.07	0.25±0.04	0.17±0.01	0.06±0.00
	2	--	0.24±0.03	0.30±0.05	0.50±0.12	0.37±0.07	0.28±0.04	0.30±0.04	0.33±0.03	0.07±0.01
30-40	1	0.03±0.00	0.21±0.05	0.35±0.06	0.49±0.09	0.48±0.12	0.34±0.09	0.25±0.07	0.14±0.01	0.06±0.00
	2	--	0.23±0.04	0.28±0.03	0.20±0.02	0.18±0.01	0.17±0.01	0.23±0.07	0.27±0.07	0.06±0.01
40-50	1	0.06±0.00	0.36±0.04	0.38±0.04	0.34±0.03	0.39±0.04	0.31±0.01	0.22±0.00	0.11±0.02	0.07±0.01
	2	--	0.23±0.13	0.23±0.07	0.16±0.15	0.17±0.10	0.15±0.05	0.20±0.00	0.27±0.01	0.05±0.01

Depth(cm)	C <sub>2 year</sub> /C <sub>1 year</sub> (%)								
	C <sub>12</sub>	C <sub>14</sub>	C <sub>16</sub>	C <sub>18</sub>	C <sub>20</sub>	C <sub>22</sub>	C <sub>24</sub>	C <sub>26</sub>	C <sub>28</sub>
0-4	--	17.06	16.93	19.53	15.48	15.96	20.50	23.16	20.45
5-8	--	43.09	42.16	44.23	47.62	46.22	46.45	40.81	31.23

---

9-12	--	46.16	25.32	28.76	23.33	23.22	23.91	46.93	84.84
13-16	--	68.75	38.96	72.00	31.32	28.40	35.89	59.59	21.75
17-20	--	102.13	206.20	254.50	190.23	156.28	161.08	174.20	15.82
21-24	--	79.38	143.61	258.77	174.76	165.83	193.80	229.65	29.16
25-30	--	76.37	68.15	90.91	91.13	76.58	120.72	197.29	114.85
30-40	--	107.28	80.25	40.26	36.87	48.52	92.32	188.52	103.10
40-50	--	64.68	59.92	46.09	43.49	50.11	91.04	242.72	61.51

---

Figure skipped

**Figure 2-6** Vertical distribution of 9 n-alkanes in aged soil box for two year aging treatment in the field

### 2.1 Changes in n-alkanes' depth redistribution in soil after field ageing

The depth distributions of C12-C28 even n-alkanes (especially C16-C26 n-alkanes) observed in the diesel-polluted soil flume after one-year field aging decreased sharply with depth (data not shown). The diesel was largely retained within surface layer (0-12cm) and only less than 10 mg/kg of individual n-alkanes were detected at soil depths greater than 12 cm. Apparently, the diesel was strongly sorbed by the soil and therefore could hardly migrate downwards to deep layers. Compared to the initial depth distributions of the diesel at the time of spiking, the concentrations of short-chain even n-alkanes (C12-C14) in the soil decreased drastically after one year of field aging while the concentrations of long-chain even n-alkanes (C16-C28) decreased slightly and still presented at relatively high concentrations (data not shown). It could be inferred that the short chain n-alkanes may dissipate easily from the soil probably via volatilization and biodegradation while the long chain n-alkanes can persist in the soil for a long period. Therefore, once the soil is accidentally contaminated by the diesel, implementation of appropriate remediation practice is definitely required in most cases.

### 2.3.2 Desorption characteristics of alkanes from soil with LAS

Figure skipped

**Figure 2-7** Desorption characteristic n-alkanes by different concentration of surfactants in batch desorption experiment

**Table 2-7** Batch desorption by surfactants in diesel-polluted soils

LAS	C <sub>12</sub>	C <sub>14</sub>	C <sub>16</sub>	C <sub>18</sub>	C <sub>20</sub>	C <sub>22</sub>	C <sub>24</sub>	C <sub>26</sub>	C <sub>28</sub>
	mg Kg <sup>-1</sup>								
0 CMC	-	0.38 <sup>a</sup>	2.19 <sup>a</sup>	5.90 <sup>a</sup>	6.21 <sup>a</sup>	4.20 <sup>a</sup>	2.35 <sup>a</sup>	1.04 <sup>a</sup>	0.75 <sup>a</sup>
1 CMC	-	0.69 <sup>a</sup>	9.14 <sup>B</sup>	25.53 <sup>B</sup>	25.83 <sup>B</sup>	17.70 <sup>B</sup>	9.19 <sup>B</sup>	3.13 <sup>B</sup>	1.18 <sup>B</sup>
3 CMC	-	1.51 <sup>B</sup>	20.84 <sup>C</sup>	57.94 <sup>C</sup>	53.47 <sup>C</sup>	34.51 <sup>C</sup>	16.42 <sup>C</sup>	5.16 <sup>C</sup>	1.29 <sup>B</sup>
5 CMC	-	3.07 <sup>C</sup>	26.93 <sup>D</sup>	68.63 <sup>D</sup>	60.52 <sup>D</sup>	37.43 <sup>C</sup>	17.44 <sup>C</sup>	5.13 <sup>C</sup>	1.38 <sup>B</sup>

a means followed by the same letter in the same row do not differ by Tukey test ( $p < 0.05$ )

100 cm<sup>3</sup> ring samples taken at different soil depths before and after the plowing treatment of the soil flume on April 15, 2014 were measured for saturated hydraulic conductivity and soil water retention curve. Following the plowing practice to the depth of 20 cm, Ks of surface soil increased by an order and differences in van Genuchten (1980) soil water retention curve were observed as shown below.

Before-plowing:

0-10 cm depth:  $\theta = 0.223 + 0.318 * (1 + (0.286 * h)^{1.361}) - 0.265$  ;

10-20 cm depth:  $\theta = 0.231 + 0.213 * (1 + (0.229 * h)^{1.199}) - 0.166$ ;

20-30 cm depth:  $\theta = 0.219 + 0.203 * (1 + (0.119 * h)^{1.264}) - 0.209$ ;

1 week after plowing:

0-10 cm depth:  $\theta = 0.224 + 0.332 * (1 + (0.147 * h)^{1.437}) - 0.304$ ;

10-20 cm depth:  $\theta = 0.244 + 0.249 * (1 + (0.147 * h)^{1.403}) - 0.287$ ;

20-30 cm depth:  $\theta = 0.223 + 0.215 * (1 + (0.163 * h)^{1.227}) - 0.185$

**Figure 2-7** Soil water retention curves-VG of initial diesel contaminated soil**Table 2-4** SWRC parameters obtained using Van Genuchten model for initial diesel contaminated soil

### 3 Effects of LAS-enhanced flushing on soil chemical properties and the leachate from soil column freshly spiked with diesel

### 3.1 Background

It was reported that higher surfactant concentrations may lead to increased colloid mobilization (Gardner and Arias 2005). Colloids could potentially act as transport vehicles for various strongly-sorbing contaminants such as heavy metals and organic contaminants (Tang et al 2012; Zhang et al. 2015, 2016). Colloid transport may not only promote the migration of contaminants but also alter soil structure and flow paths in the subsurface (Zhang et al. 2015). The interactions between surfactants and soil matrix may exert substantial effects on soil pore system as a result of colloid transport.

In-depth understanding of the impact of soil flushing treatment on properties is critically important. There is a lack of integrated research which can relate the chemical changes in soil chemical properties and the leachate from soil column freshly spiked with diesel upon surfactant-enhanced soil flushing treatment.

### 3.2 Materials and Methods

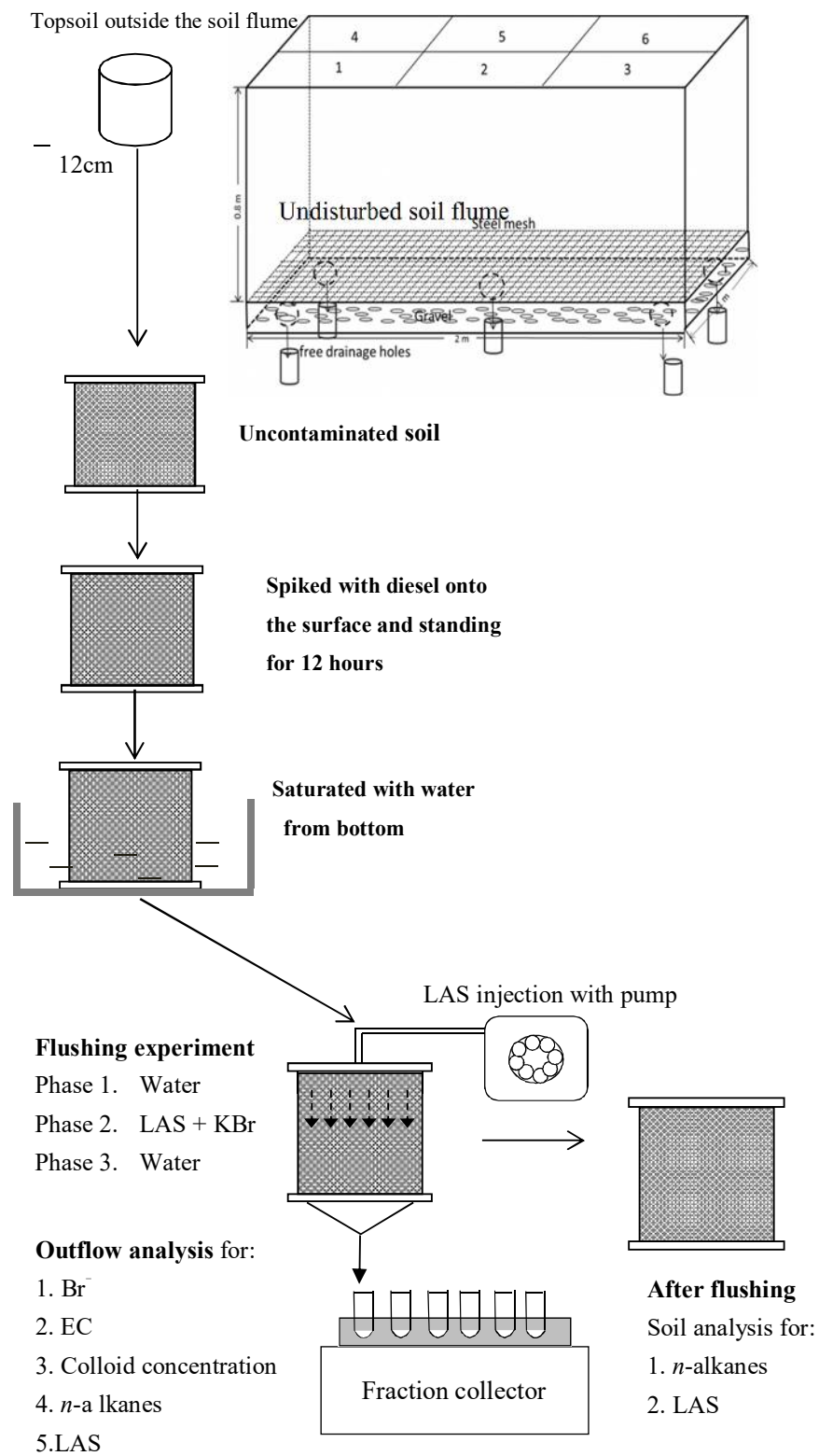


**Figure 3-1** Experimental scheme of the study

- 3.2.1 Preparation of repacked soil columns
- 3.2.2 Diesel spiking and soil column flushing with LAS
- 3.2.3 Analysis of column outflow and flushed soil
- 3.3 Results and Discussion

Figure skipped

- 3.3.1 Dynamics of LAS and alkanes in column outflow

Figure skipped

**Figure 3-2.** Breakthrough curves for topsoil column with freshly added diesel of 9 n-alkanes in the soil flushing experiments

Figure skipped

**Figure 3-3** Breakthrough curves for topsoil column with freshly added diesel of LAS (C<sub>10</sub>-C<sub>13</sub> homologues) in the soil flushing experiments.

Figure skipped

**Figure 3-4** Breakthrough curves for topsoil column with freshly added diesel of colloid, Br<sup>-</sup>, LAS, n-alkanes and EC in the soil flushing experiments.

Fractures simulations involving transport through fracture networks in a clay and a sandstone

rock indicate that colloid-facilitated contaminant transport can be an important factor leading to the rapid exceedance of water quality standards at large distances from the contaminant source. If the colloids are highly mobile in open fractures and there is a strong affinity for a reactive contaminant to remain adsorbed onto them, then low but environmentally significant contaminant concentration levels can quickly propagate through an interconnected network of fractures.

One of their conclusions was that if contaminant desorption from the mobile colloids is a slow kinetic process, then the presence of the colloids can lead to significantly enhanced contaminant migration.

Colloids can be highly mobile over significant distances in fractured soils and subsoils derived from clay-rich materials including saprolite (decomposed materials that retain the fabric of the parent bedrock), glacial till, and other sedimentary deposits. Other laboratory- or small-scale field tracer experiments also show that colloids can be transported rapidly in clay-rich fractured or macropore-dominated soils and that loss or retention rates can widely vary (1-7). These studies suggest that colloidal contaminants, such as pathogenic microorganisms or radionuclides attached to colloidal particles (8), may also be mobile in fractured clay-rich deposits and could adversely impact underlying aquifers or nearby streams.

### **Transport dynamics of diesel alkanes, LAS and colloids through soil column**

Undisturbed soil columns taken at the 0-12 cm were flushed with LAS and the dynamics of the chemical composition and colloidal properties in effluent were obtained. The results showed that, *n*-alkanes (C<sub>12</sub>-C<sub>28</sub>) discharge was enhanced by LAS flushing, as compared to water flushing.

3.3.2 Removal of alkanes from soil and depth distributions of alkanes and LAS residues in soil

Soil column flushing with surfactants

Undisturbed soil columns taken at the 0-12 cm (column A1) and 12-24 cm (column B1) depth

were flushed with LAS and the residue n-alkanes (C<sub>12</sub>-C<sub>28</sub>) of each column were detected after flushing experiment for different soil layers (each 4 cm in depth). Column A0 which represent the undisturbed soil column with diesel freshly added.

As freshly added diesel (Column A0), the results of showed that (Table 3-1), LAS flushing could not only promote the transportation but also enhance the vertical distribution of n-alkanes which lead to decrease the surface concentration and increase the middle and bottom of residue n-alkanes in the freshly contaminated column.

Following the plowing practice to the depth of 20 cm, Ks of surface soil increased by an order and differences in van Genuchten (1980) soil water retention curve were observed as shown below.

Figure skipped

**Figure 3-5** Depth distributions of LAS residues (C<sub>10</sub>-C<sub>13</sub> homologues) in topsoil column with freshly added diesel columns after LAS-enhanced flushing

(1) Study of the temporal variation and vertical migration characteristics of N-alkanes in diesel-polluted soils.

Comparing diesel-polluted purple soils which had been aged for the 1 month and 6 months in the laboratory, the concentration of short-chain even N-alkanes (C<sub>12</sub>-C<sub>16</sub>) decreased greatly, but the concentration of the long-chain even n-alkanes (C<sub>18</sub>-C<sub>28</sub>) did not change significantly at the initial diesel addition level of both 10 g/kg and 50 g/kg. Similarly, the concentrations of short-chain even n-alkanes (C<sub>12</sub>-C<sub>16</sub>) in the soils after 1 year aging in the field condition decreased drastically while the long-chain even n-alkanes (C<sub>18</sub>-C<sub>28</sub>) decreased slightly and still presented at relatively high concentrations. These observations suggest that the short chain n-alkanes dissipated from the soils probably via volatilization and biodegradation. The depth distribution of n-alkanes in the undisturbed diesel-polluted soil flume was analyzed. The result showed that most of n-alkanes stayed in the surface layer (0-12cm) and hardly migrated downwards to greater depths.

(2) The batch desorption experiments by surfactants in diesel-polluted soils.

Desorption experiments showed that seven critical micelle concentration (CMC) of LAS (C10-C13) exhibited highest removal efficiency for n-alkanes from diesel-contaminated soils aged for 1 year in the field and higher LAS concentrations did not lead to significantly greater removal efficiencies of diesel.

(3) Flushing experiments of undisturbed columns with surfactants under constant flux.

Undisturbed soil columns (15 cm in diameter, 12 cm in length) taken at the 0-12 cm and 12-24 cm depth of the 1 year aged soil flume were flushed with LAS and the dynamics of the chemical composition and colloidal properties in effluent were determined. The result showed that, n-alkanes (C12-C28) discharge was enhanced by LAS flushing, as compared water flushing. In particular, the removal efficiency could reach 95% for long-chain n-alkanes. The colloid concentrations in the effluent during LAS flushing were about 100 times higher than that during water flushing. It seemed that the LAS molecular could interact with soil particles and thus mobilize colloids that could migrate through macropores in the purple soil. It should also be noted that high concentrations of colloids might lead to pore plugging to some extent in the middle layer of the soil column, resulting in the observed high LAS residue in the middle of the column than in the surface layer.

**Table 3-1** The n-alkanes residue for topsoil column with freshly added diesel after soil flushing experiments

	concentration		C <sub>14</sub>	C <sub>16</sub>	C <sub>18</sub>	C <sub>20</sub>	C <sub>22</sub>	C <sub>24</sub>	C <sub>26</sub>	C <sub>28</sub>
0-4cm	Flushed	mg Kg <sup>-1</sup>	443.98	547.02	532.15	356.40	193.32	87.48	24.24	5.52
5-8cm	Flushed	mg Kg <sup>-1</sup>	194.49	283.55	300.55	216.23	120.29	53.77	14.28	3.13
9-12cm	Flushed	mg Kg <sup>-1</sup>	17.73	24.25	26.12	18.99	11.37	5.57	2.07	0.49

### 3.4 Conclusions

## 4 Effects of LAS-enhanced flushing on packed soil columns

### 4.1 Background

### 4.2 Materials and Methods

The packed soil column was pre-wetted with  $0.5 \text{ g L}^{-1} \text{ NaN}_3$  solution from the bottom, prior to flushing experiment, to fill the empty pores and inhibit biodegradation. After complete water saturation, five pore volumes (PV) of water (containing  $0.5 \text{ g L}^{-1} \text{ NaN}_3$ ) were supplied from the bottom the eliminate gravity , using a peristaltic pump at a flow rate of  $0.3 \text{ mL/min}$ , from the bottom of the top to establish a steady hydro-physical and chemical equilibrium between injection solution and soil matrix. Afterwards, the column was flushed with 8-12 PV of water or  $1.98 \text{ g L}^{-1}$  LAS (3 CMC )solution containing. The outflow was continuously collected in 10 mL each sample by a fraction collector. Outflow samples were analyzed for pH, EC zeta potential and particle size distribution.

#### 4.2.1 Preparation of repacked columns with diesel-polluted soil

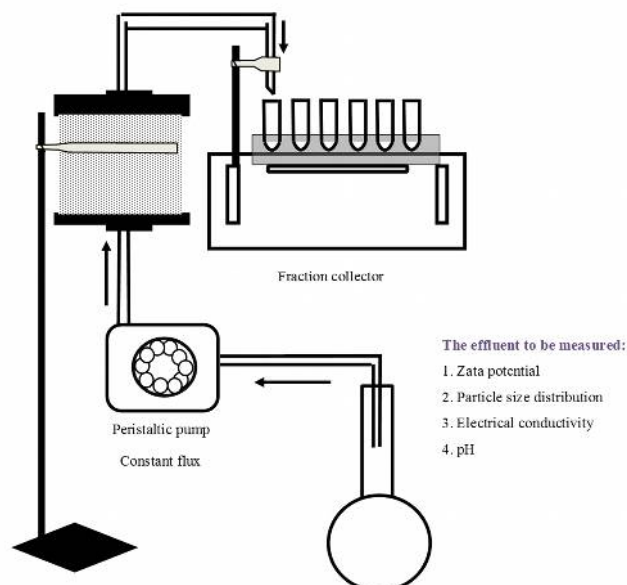


**Figure 4-1** Experimental scheme of the study

#### 4.2.2 Soil flushing with LAS and analysis of column outflow

### 4.3 Results and Discussion

#### 4.3.1 Particle size distribution in column outflow

#### **Figure skipped**

**Figure 4-2** Chemical properties of outflow samples for packed column in representative collected at different flushing phases. (a) Topsoil packed column with water flushing (b) Topsoil packed column with LAS flushing

Colloid transport experiments through repacked soil columns (3 cm in diameter, 5cm in length) were conducted to investigate the effect of LAS flushing on colloid release from diesel-polluted soils under constant flux. Compared to the mean diameter of colloids (about 10-20 nm) observed during water flushing, larger sizes of colloids in the effluents during LAS injection, with the mean diameter of colloids being 600-800 nm, were detected. During LAS injection, the colloids were more negatively charged (i.e., lower Zeta potential), which made them better dispersed and more stable and colloids of larger sizes can be mobilized and transported.

#### **Figure skipped**

**Figure 4-3** Chemical properties of outflow samples for packed column in representative collected at different flushing phases. (a) Subsoil packed column with water flushing (b) Subsoil packed column with LAS flushing

#### **Figure skipped**

**Figure 4-4** Particle size distributions of colloids in representative outflow samples collected at different flushing phases. (a) Topsoil packed column with water flushing or LAS flushing (b) Subsoil packed column with water flushing or LAS flushing

## **5 Effects of LAS-enhanced flushing on transport of colloids and solutes and various soil properties of diesel-polluted soil after one-year ageing**

### **5.1 Background**

Although surfactants-enhanced flushing technique is generally efficient to clean up soil, the major concern remains because of mixed results of its application in soil matrix (Urum et al. 2006). During the surfactant-enhanced soil flushing treatment, various interactions between the soil and surfactant solution may take place and lead to changes in soil hydraulic properties and other potential environmental consequences (Renshaw et al. 1997; Jia et al. 2005; Laha et al. 2009). For example, hydraulic conductivity reduction was observed in the loamy soils (Gabr et al. 2011); immediate plugging of soil columns followed surfactant injection (Roy et al. 1995). Contrastingly, some other researches have shown that, extensive soil column tests achieved high oil recoveries exceeding 99% without significant problems such as pore clogging and high surfactant retention (Dwarakanath and Pope 2000). Notably, it was reported that higher surfactant concentrations may lead to increased colloid mobilization (Gardner and Arias 2005). Colloids could potentially act as transport vehicles for various strongly-sorbing contaminants such as heavy metals and organic contaminants (Tang et al 2012; Zhang et al. 2015, 2016). Colloid transport may not only promote the migration of contaminants but also alter soil structure and flow paths in the subsurface (Zhang et al. 2015). The interactions between surfactants and soil matrix may exert substantial effects on soil pore system as a result of colloid transport.

Soil structure governs various important physical and biological processes in soil-plant-microbial systems (Martinez et al. 2010; Garbout et al. 2013). For soils that have poor structures and are weakly aggregated, in addition to the contaminant removal efficiency of surfactant-

enhanced flushing technology, due attention should be paid to the colloid-associated contaminant export with the flushing outflow as well as resulting changes in soil pore character. However, to our knowledge, few relevant investigations have been conducted with undisturbed columns of contaminated soils aged in the field. For example, in the vast hilly region (160,000 km<sup>2</sup>) of Sichuan in the upper Yangtze River, poorly structured purple soil (an entisol according to USDA soil taxonomy) shows a high potential to release colloids in the subsurface upon rainfall (Zhang et al. 2015). Therefore, the feasibility of applying surfactant-enhanced flushing technology in this region for soil remediation needs to be evaluated with respect to colloid transport and soil porosity (particularly water-conducting large pores).

The visualization and quantification of macropores are essential for a better understanding of soil structure. In recent years, X-ray micro-computed tomography (Micro-CT) scanning has been employed to study the characteristics of soil macropores, which is known as a nondestructive and powerful technique to visualize and quantify the characteristics (e.g. number, size and location) of soil macroporosity (Lamande et al. 2013; Wang et al. 2016). There have been no previous studies using this advanced technique to directly quantify the effects of surfactant-enhanced flushing treatment on water conducting macropores.

The objective of this study is to gain new insights into adverse impacts of LAS-enhanced flushing for purple soil, using undisturbed columns of diesel-contaminated farmland soil aged in the field for one year, with special regards to colloid transport and soil macroporosity. The results of this study could also be supportive to full evaluation of the feasibility of this soil remediation technique for field application in not only this studied entisol but also other poorly structured, aggregated soils.

## 5.2 Materials and Methods

### 5.2.1 LAS-enhanced flushing experiment through columns of field aged diesel-polluted soil

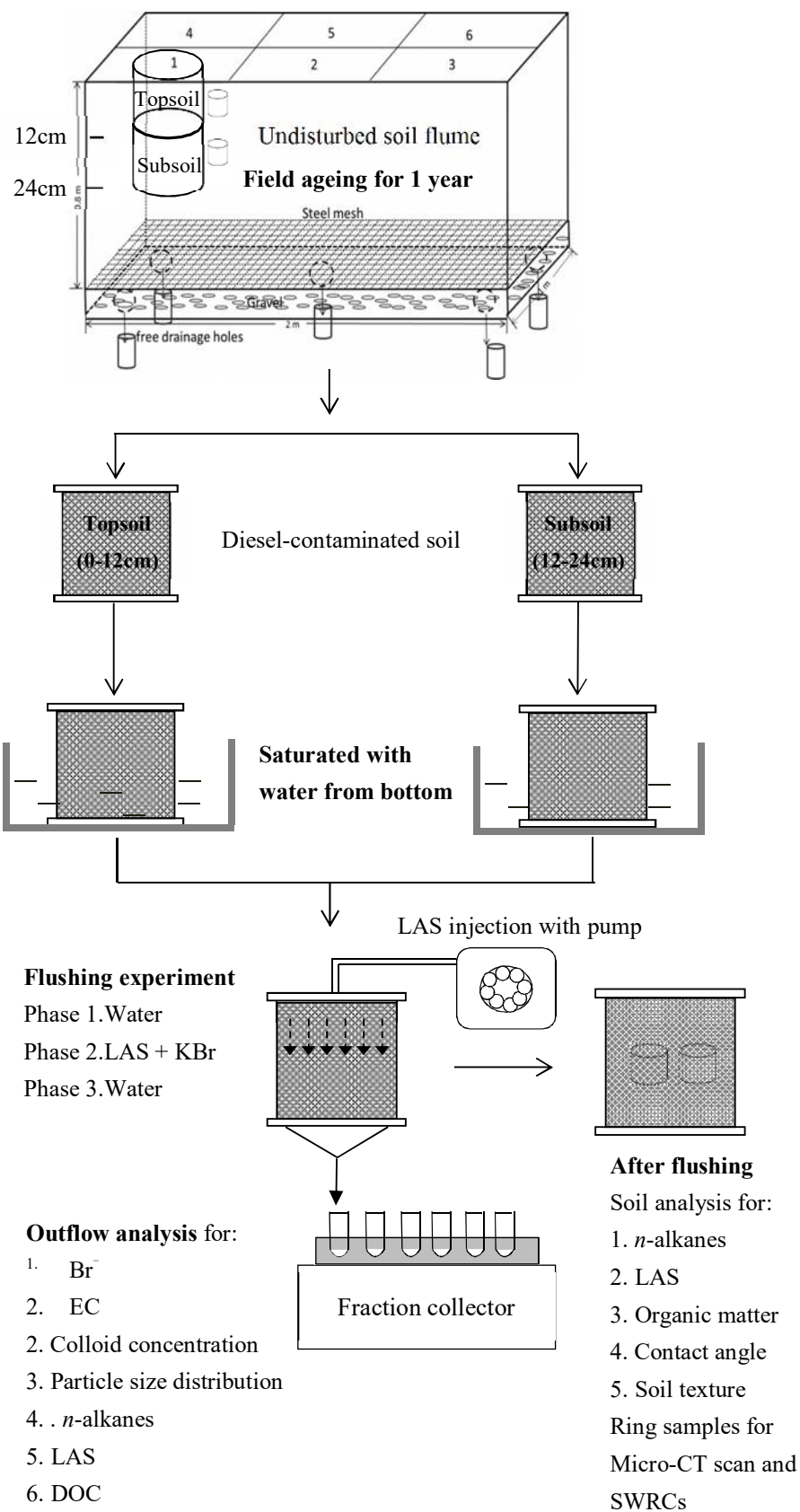


**Figure 5-1** Experimental scheme of the study.

## Flushing experiments

The intact soil column was pre-wetted with  $0.5 \text{ g L}^{-1} \text{ NaN}_3$  solution from the bottom, prior to flushing experiment, to fill the empty pores and inhibit biodegradation. After complete water saturation, five pore volumes (PV) of water (containing  $0.5 \text{ g L}^{-1} \text{ NaN}_3$ ) were supplied, using a peristaltic pump at a flow rate of  $8 \text{ mL/min}$ , from the top of the column to establish a steady hydro-physical and chemical equilibrium between injection solution and soil matrix (phase 1). Afterwards, the column was flushed with 3 PV of  $1.98 \text{ g L}^{-1}$  LAS solution containing KBr ( $50 \text{ mg-Br L}^{-1}$ , a non-reactive tracer) (phase 2), followed by 4 PV of water (containing  $0.5 \text{ g L}^{-1} \text{ NaN}_3$ ) (phase 3). This LAS concentration, equivalent to three times of measured critical micelle concentration of LAS ( $\text{C}_{10}\text{-C}_{13}$ ), was used because it led to sufficiently high removal efficiencies for *n*-alkanes in preliminary batch desorption experiments. The outflow was continuously collected in 50 mL each sample by a fraction collector. Outflow samples were analyzed for  $\text{Br}^-$ , colloid concentration and particle size distribution. After completing all three phases of flushing, the soil column set was dismantled and carefully sampled every 4 cm in depth for analysis of diesel and LAS residues in the flushed soil. Meanwhile, two small intact soil ring samples (5 cm in diameter, 5 cm in length) were taken from the middle part of the flushed column and examined for soil macropores exhaustively using an industrial Phoenix Nanotom X-ray micro-CT (GE, Sensing and Inspection Technologies, Germany).

### 5.2.2 Analysis of column outflow and flushed soil

#### 5.3.1 Dynamics of EC, LAS, alkanes and particle size distribution in column outflow

The original outflow samples were analyzed for *n*-alkanes, LAS, colloid concentration and particle size distribution.  $\text{Br}^-$  concentration was determined with  $0.45 \text{ }\mu\text{m}$ -filtered outflow samples.

The concentration of  $\text{Br}^-$  was determined using a modified version of method 4500- $\text{Br}^-$  B with a detection limit of  $0.01 \text{ mg L}^{-1}$  (American Public Health Association, 1995). Colloid concentration was determined spectrophotometrically (Tu-1810, Purkinje General Instrument Co., Beijing, China) at a wavelength of 400 nm using a previously established calibration curve of the colloid concentration ( $0\text{-}2000 \text{ mg L}^{-1}$ ) vs. absorbance. The absorbance measured in

filtered outflow, probably as a result of the formation of emulsion in the presence of LAS, was deducted from that measured in unfiltered outflow. The detection limit for colloids was 1 mg L<sup>-1</sup>. Particle size distribution (PSD) was determined in the 15 mL fraction cell without ultrasound treatment or dilution by a laser scattering particle size distribution analyzer (LA950, Horiba, Ltd., Kyoto, Japan).

### **Soil analysis**

Nine even *n*-alkane homologues (C<sub>12</sub>-C<sub>28</sub>) which were chosen to represent the main saturated hydrocarbons constituting the diesel used in this study. Methods for sample pretreatment and analysis were optimized. Soil samples were pretreated by ultrasonic-assisted dispersive solid phase extraction with activated carbon clean-up method prior to analysis for gas chromatography with a flame ionization detector (7890A GC-FID, Agilent, USA), an Agilent autosampler and Agilent 19091J-413 column (30 m×0.32 mm i.d.) with a nominal film thickness of 0.25 μm. The detailed procedure for sample pretreatment was: 2 g of soil sample was extracted by 10 mL of hexane mixed with 5 g of anhydrous sodium sulfate in a ultrasonic device (at 300 W) for 90 min and the extract was filtered through a 0.45-μm polyamide filter membrane after centrifugation, the filtrate was purified with 0.01g of activated carbon and filtered through 0.45 μm. The filtrate was then concentrated to near dryness in a rotary evaporator (BUCHI, Switzerland) and then 1 mL of hexane (Merck KGaA, Germany) was added to dissolve the target compounds for subsequent analysis with the GC-FID. The injector and detector temperatures were set at 250 and 330°C, respectively. N<sub>2</sub> was used as carrier gas at a flow rate of 1 mL min<sup>-1</sup>. The column temperature was programmed as follows: increased from 70°C (held for 2 min) to 300°C at 4°C min<sup>-1</sup> and then held at 300°C for 5 min. 2 μL of the sample was injected manually in the splitless mode. The detection limits were 0.01-0.05 mg L<sup>-1</sup> for C<sub>12</sub>-C<sub>28</sub> *n*-alkanes.

Four LAS homologues (C<sub>10</sub>-C<sub>13</sub>) were chosen to represent the principal components of the commercial LAS mixture supplied by Sigma-Aldrich. Soil sample was pretreated by ultrasonic-assisted dispersive solid phase extraction using activated carbon and SPE clean-up method prior to analysis by liquid chromatography with a UV detector at 275 nm (1260 Infinity HPLC-UV, Agilent, USA). Chromatographic separation was performed by a Symmetry C8 column (150

mm  $\times$  4.6 mm i.d. with 5  $\mu$ m film thickness) (Angilent, USA) with security guard column. The mobile phase used in the chromatographic separation at a flow rate of 0.5 mL min<sup>-1</sup> consisted of a binary mixture of methanol and water (78:22) containing 0.5 mmol L<sup>-1</sup> sodium acetate. The column temperature was set at 30°C. 1  $\mu$ L of the sample was injected with automatic sampling device. The detection limits were 0.02-0.03 mg L<sup>-1</sup> for C<sub>10</sub>-C<sub>13</sub> LAS.

Small intact soil cores, which were taken under moist conditions (0.33-0.38 cm<sup>3</sup> cm<sup>-3</sup>) from the unflushed soil box placed in the field and the soil columns flushed in the laboratory for comparison, were scanned by X-ray micro-CT. The beam hardening effect was reduced using a 0.2 mm Cu filter. The scanning was performed using a voltage of 120 kV and an exposure of 350 mAs. The filtered back-projection algorithm was used to reconstruct the images. Two thousand slices with size 1052  $\times$  1052 pixels, stored in 8-bit format, were produced for each core sample. The resulting voxel size was 30  $\times$  30  $\times$  30  $\mu$ m<sup>3</sup>.

A maximal ball algorithm developed by Dong (2007) was used to extract topologically equivalent networks of pores and throats so that 3D micro-CT images derived from their original 2D images could be used as input to pore network models. Various pore structure parameters, such as the volumes, numbers and shape factors of the pores and throats, aspect ratio, were calculated as described by Dong (2007) to evaluate the effects of LAS-enhanced flushing on soil macropores that can be captured by the Micro-CT scanner.

### **Effects of LAS-enhanced flushing on colloid transport through soil column**

Breakthrough curves of Br<sup>-</sup> through topsoil and subsoil columns during flushing experiments are shown in Figure 2. The dramatic decline in outflow Br<sup>-</sup> concentration took place in a much shorter time after switching from LAS flushing to water flushing for the topsoil column, as compared to the subsoil column. This indicates that more significant preferential flow through macropores occurred in the topsoil column while matrix flow's contribution to column outflow was much higher for the subsoil.

### Figure skipped

**Figure 5-2** Breakthrough curves of Br<sup>-</sup> through undisturbed columns of diesel-contaminated topsoil (solid circles) and subsoil (solid triangles). At PV = 0, flushing solution was switched from water to LAS. Vertical dashed lines indicate the times of switching from LAS flushing to final water flushing.

It was reported that LAS could promote the release of soil colloids (Park et al. 2005) and the colloidal particles transported through macropores during flushing may lead to pore clogging in soil column (Du et al. 2013). The results of the present study showed that surfactants could lead to high export of colloid transport through soil columns (Figure 3). Compared to the outflow of initial and final water flushing, colloid discharge from the column was significantly higher during LAS flushing. The release of colloids could be attributed to enhanced soil colloid dispersion by LAS. Similar phenomena were reported (Gardner and Arias et al. 2000; Du et al. 2013). Colloid discharge from the topsoil column was much larger and slower than the subsoil column, indicating there was a larger pool of colloids in the subsoil that can be more easily dispersed by LAS. During final water flushing, colloid concentrations in the outflow from the topsoil column were higher than the subsoil column, indicating colloids could be more water dispersible in the topsoil. This phenomenon implies that clogging of small pores by fine colloids was more likely to take place for the topsoil during final water flushing.

### Figure skipped

**Figure 5-3** Breakthrough curves of colloids through undisturbed columns of diesel-contaminated topsoil (solid circle) and subsoil (solid triangle). At PV = 0, flushing solution was switched from water to LAS. Vertical dashed lines the times of switching LAS flushing to final water flushing.

Representative colloidal particle size distributions in the outflow from the columns during three flushing phases are shown in Figure 5. Compared to initial and final water flushing phase, larger sizes of colloids were detected in the outflow during LAS flushing phase. The maximum

diameter of colloidal particles could be up to 1500  $\mu\text{m}$  during LAS flushing while was basically less than 100  $\mu\text{m}$  during water flushing. Higher proportions of large size colloids were observed during LAS flushing for the topsoil column, indicating colloids were transported mainly through macropores given its more solid evidence of preferential flow than the subsoil column from  $\text{Br}^-$  breakthrough curves. This is further corroborated by the results of micro-CT scanning described below.

### Figure skipped

**Figure 5- 4** Particle size distributions of colloids in representative outflow samples collected at different flushing phases. (a) Topsoil column (outflow samples collected at 5 PV initial water flushing, 2.5 PV LAS flushing and 3 PV final water flushing); (b) subsoil column (outflow samples collected at 6 PV initial water flushing, 3 PV LAS flushing and 1 PV final water flushing).

### Figure skipped

**Figure 5-4** Breakthrough curves of 9 n-alkanes through undisturbed columns of diesel-contaminated topsoil (solid circle) and subsoil (solid triangle). At PV = 0, flushing solution was switched from water to LAS.

### Figure skipped

**Figure 5-3** Breakthrough curves of LAS ( $\text{C}_{10}$ - $\text{C}_{13}$  homologues) through undisturbed columns of diesel-contaminated topsoil (solid circle) and subsoil (solid triangle). At PV = 0, flushing solution was switched from water to LAS. Vertical dashed lines the times of switching LAS flushing to final water flushing.

### Figure skipped

**Figure 5-3** Breakthrough curves of colloids, Br<sup>-</sup>, Total LAS and EC through undisturbed columns of topsoil (A) and subsoil (B) column. At PV = 0, flushing solution was switched from water to LAS. Vertical dashed lines the times of switching LAS flushing to final water flushing.

#### 5.3.2 Effects on soil hydraulic properties

SWRCs were determined in the laboratory by using a sand-kaolin box (Romano et al., 2002). SWRCs were determined in the pressure range  $h = 0$  down to -200 cm, since it was already recognised that tillage effects on pore space are more pronounced in that  $h$ -range (Lindstrom and Onstad, 1984; Mapa et al., 1986; Poulouvassilis, 1990). For obtaining the SWRCs representing each plot at the sampling date,  $\theta_i(h)$  values were used, where  $\theta_i$  was the average of the five measured  $u$  values prevailing on the five samples, extracted for the five sampling sites of each plot, at a given  $h$  value. The analytic expression for the SWRC of van Genuchten (1980) was fitted to the experimental data using the code RETC (van Genuchten et al., 1991). The van Genuchten equation is

$$\frac{\theta - \theta_r}{\theta_s - \theta_r} = \Theta = \frac{1}{[1 + (-\alpha h)^n]^m}$$

Where  $\theta$  = volumetric soil water content (cm<sup>3</sup>/cm<sup>3</sup>);  $h \leq 0$  = soil water pressure head (cm);  $\theta_r$  = residual volumetric soil water content (cm<sup>3</sup>/cm<sup>3</sup>).  $\theta_s$  = volumetric soil water content at zero pressure head (cm<sup>3</sup>/cm<sup>3</sup>).

$a$  (cm<sup>-1</sup>),  $n$  and  $m$  are positive fitting parameters ( $a > 0$ ,  $n > 1$ ,  $m = 1 - 1/n$ ).

$\Theta$  = The effective saturation.

The water retention data from were measured in the range  $10 < h < 15000$  hPa on the drying

limbs of the water retention characteristics. The data were fitted to the water retention equation of Dexter et al. (2008)

$$W = C + A_1 e^{-h/h_1} + A_2 e^{-h/h_2}$$

The fitting was done using the Marquardt–Levenberg algorithm (Marquardt, 1963). In Eq. (1),  $w$  is the gravimetric water content which is expressed as a function of soil water suction (or matric potential),  $h$ . The first term,  $C$ , is the asymptotic value of  $w$  as  $h \rightarrow \infty$  which can be described as the residual water content. The second term with  $A_1$  and  $h_1$  describes the matrix porosity, whereas the third term with  $A_2$  and  $h_2$  describes the structural porosity. The values of  $A$  give the amounts of the pore spaces, whereas the values of  $h$  give the effective cylindrical diameters,  $\delta$ , of the pores through the equation

**Table 5-1** SWRC parameters obtained using Van Genuchten and Bi-exponential model

Treatment	Uncontaminated		Diesel-contaminated, aged		LAS flushed		
	Topsoil	Subsoil	Topsoil	Subsoil	Topsoil	Subsoil	
pH	8.52	8.47	8.16	8.37	8.17	8.75	
OM	13.53	13.91	22.23	14.53	17.64	15.33	
Contact angle	58.46	68.93	43.89	63.29	50.02	61.50	
van Genuchten (1980) model	$\theta_r$	0.22	0.24	0.16	0.19	0.16	0.30
	$\theta_s$	0.56	0.49	0.57	0.49	0.51	0.47
	$n$	1.44	1.40	1.22	1.19	0.18	0.16
	$\alpha$	0.15	0.15	1.69	1.22	1.00	2.86
	$m$	0.30	0.29	0.18	0.16	0.10	0.04
Bi-exponential model (Ref)	$\theta_{r-BE}$	0.24	0.26	0.20	0.24	0.28	0.30
	$\theta_{txt}$	0.09	0.07	0.11	0.08	0.09	0.07
	$h_{a-txt}$	653.60	745.50	916.61	1052.21	1168.90	4187.31
	$\theta_{str}$	0.22	0.16	0.32	0.18	0.14	0.09
	$h_{a-str}$	24.85	23.1	4.03	6.60	10.28	13.53

**Figure skipped**

Fig. (a), (b) Soil water retention curves-VG (c),(d) Soil water retention curves-BE

**Figure skipped**

### **Diesel removal from soil column by LAS-enhanced flushing**

Since flushing experiments showed similar results of diesel removal among triplicate columns for both topsoil and subsoil, only the results for one topsoil column (0-12 cm) and one subsoil column (12-24 cm) are presented in this article. Measured depth distributions of *n*-alkanes (C<sub>12</sub>-C<sub>28</sub>) residues and removal for the two soil columns after LAS-enhanced flushing are shown in Table 2. The removal rate varied with soil depth and was highest in the middle layer (4-8 cm) of topsoil columns. The maximum removal rate of 96% was observed for C<sub>18</sub> *n*-alkanes, which could be caused by the highest residual LAS concentration observed in the middle layer. For the subsoil at low diesel contamination level, no residual *n*-alkanes were detected after flushing. Effective removal (88%) of diesel by in situ flushing with nonionic surfactant (2% sorbitan monooleate solution) was reported at a contaminated site (Lee et al. 2005)

**Table 2** The *n*-alkanes removal in diesel-contaminated soils after LAS-enhanced flushing

Depth (cm)			C <sub>14</sub>	C <sub>16</sub>	C <sub>18</sub>	C <sub>20</sub>	C <sub>22</sub>	C <sub>24</sub>	C <sub>26</sub>	C <sub>28</sub>	
Topsoil column	0-4	Before flushing	mg kg <sup>-1</sup>	6.46	66.03	226.59	139.34	68.00	30.54	7.60	1.37
		After flushing	mg kg <sup>-1</sup>	1.94	13.93	79.83	69.41	50.41	26.13	6.91	0.90
		Removal rate	%	70.00	78.91	32.67	50.18	25.87	14.44	9.20	34.52
	4-8	Before flushing	mg kg <sup>-1</sup>	4.71	43.61	159.19	78.14	47.09	21.48	6.25	1.02
		After flushing	mg kg <sup>-1</sup>	1.03	2.55	6.41	5.92	4.13	2.34	0.91	0.25
		Removal rate	%	78.16	94.16	95.97	92.43	91.22	89.12	85.45	75.80
	8-12	Before flushing	mg kg <sup>-1</sup>	0.87	7.35	40.15	25.78	18.57	9.59	2.85	0.44
		After flushing	mg kg <sup>-1</sup>	0.36	1.52	3.12	2.61	1.86	1.37	0.65	0.28
		Removal rate	%	59.19	79.26	92.23	89.88	89.97	85.66	77.09	36.70
Subsoil column	12-16	Before flushing	mg kg <sup>-1</sup>	0.36	1.47	4.26	5.30	3.95	2.19	0.73	0.43
		After flushing	mg kg <sup>-1</sup>	ND	ND						
		Removal rate	%	100	100	100	100	100	100	100	100
	16-20	Before flushing	mg kg <sup>-1</sup>	0.35	0.45	0.77	0.75	0.65	0.42	0.22	0.65
		After flushing	mg kg <sup>-1</sup>	ND	ND						
		Removal rate	%	100	100	100	100	100	100	100	100
	20-24	Before flushing	mg kg <sup>-1</sup>	0.33	0.52	0.93	0.94	0.72	0.43	0.22	0.49
		After flushing	mg kg <sup>-1</sup>	ND	ND						
		Removal rate	%	100	100	100	100	100	100	100	100

ND

means the concentrations of *n*-alkanes are below the detection limits

### 5.3.3 Effects on soil macroporosity (Micro-CT 结果)

#### 2.1 Effects of LAS-enhanced flushing on soil macroporosity

Analysis of reconstructed 3D Micro-CT images (not shown) provides useful quantitative information about the impacts of LAS-enhanced flushing on soil macroporosity. Results of selected parameters of soil macropore structure are given in Table 3 and macropore size distribution shown in Figure 6. Soil macroporosity exhibited significant differences between unflushed and flushed soils. The total porosity (i.e.,  $>30\ \mu\text{m}$  macropores), number, total volume of pores and throats decreased markedly after flushing. In particular, the percentage of the  $<250\ \mu\text{m}$  macropores was lower in flushed soils than unflushed soils (Figure 6). This apparent phenomenon of soil pore blocking can be attributed to significant pore filling with colloids released in elevated quantity at the presence of LAS. Shape factor is another parameter describing soil pore and throat structure, the more irregular the pore or throat shape (i.e., lower shape factor), the more unfavorable to water and solute transport through pores or throats. After flushing, pore and throat shapes became more irregular, probably as a result of enhanced pore filling or clogging with better mobilized colloids. In particular, the proportion of fine macropores ( $<250\ \mu\text{m}$ ), which was the dominant size fraction ( $>80\%$  of the total macroporosity), decreased after LAS-enhanced flushing.

**Table 3** Selected parameters of macroporosity captured with Micro-CT scanning in the topsoil and subsoil columns before and after LAS-enhanced flushing

Soil sample	Total porosity (m <sup>3</sup> m <sup>-3</sup> )	Number of pores	Total volume of pores (μm <sup>3</sup> )	Pore shape factor	Number of throats	Total volume of throats (μm <sup>3</sup> )	Throat shape factor	Aspect ratio
Topsoil before flushing	0.05	35170	1.86×10 <sup>12</sup>	0.79	1438	4.98×10 <sup>8</sup>	0.36	0.08
Topsoil after flushing	0.01	10950	6.50×10 <sup>11</sup>	0.72	987	2.46×10 <sup>8</sup>	0.31	0.15
Subsoil before flushing	0.07	25311	2.28×10 <sup>12</sup>	0.79	515	3.98×10 <sup>8</sup>	0.31	0.04
Subsoil after flushing	0.01	9398	5.07×10 <sup>11</sup>	0.76	275	1.22×10 <sup>8</sup>	0.25	0.06

**Figure skipped**

**Figure 6** Micro-CT derived macropore size distributions in the topsoil and subsoil columns before and after LAS-enhanced flushing

		Percentage (%)					
		0.00- 0.18	0.18- 0.36	0.36- 0.54	0.54- 0.72	0.72- 0.90	>0.90
macropores	A1- contaminated	3.27	4.71	5.09	6.58	63.08	17.27
	A1-flushed	2.55	4.74	5.98	8.47	63.57	14.69
	B1- contaminated	2.88	4.63	4.73	6.79	64.83	16.14
	B1-flushed-A	6.51	5.04	3.96	6.53	63.48	14.47
macropores throat	A1- contaminated	56.68	13.70	7.30	4.73	1.11	16.48
	A1-flushed	58.59	13.85	6.18	4.47	1.41	15.51
	B1- contaminated	60.58	13.01	6.02	7.38	0.78	12.23
	B1-flushed-A	75.27	6.55	3.27	3.64	0.73	10.55

It was reported that the introduction of surfactants into soil could result in changes in water conductivity as a result of chemical reactions (Liu and Roy1995; Gabr et al. 1998), migration and subsequent deposition or straining of fine particles dispersed by surfactants in the pore network (Pennell et al. 1993). In our study, the use of LAS flushing could promote *n*-alkanes removal and increase colloid release and transport for the purple soil. It should be noted that elevated concentration of colloids may led to pore clogging to some extent, particularly in the middle layer of soil column.

Despite the limited numbers of intact columns and small cores used for LAS-enhanced flushing experiment and Micro-CT scanning, findings by different methods (e.g., enhanced colloid dispersion and transport, reduced fine macropores) in this study were consistent with each other and could be mutually corroborated. Future tests at field scales, for example in lysimeters and experimental plots with injection and extraction wells, are highly desirable to fully understand the potential environmental consequences of applying surfactant-enhanced flushing technique under varying field conditions.

Table .The shape factor of average pore

5.3.4 Effects on other soil properties (分层土有机质、接触角、机械组成和矿物组成)

## **2.2 LAS residues in soil column after flushing treatment**

Concentrations of residual LAS in the flushed soil columns are shown in Figure 5. It was found the addition of LAS resulted in not only enhanced colloid release but also the formation of emulsion (i.e., oil-LAS drops). LAS solution was injected from the top of the column during flushing experiment and the highest concentration of residual LAS sorbed to soil were expected to occur at the top layer of the column. However, this depth distribution pattern of LAS did not occur in this study. The highest residual LAS content was observed actually in the middle layer of flushed soil columns. A plausible interpretation for this phenomenon is:

LAS could be retained in colloid-associated forms through colloid filling in fine macropores as well as micropores in soil matrix; as colloids migrated downwards, more and more colloids deposited and accumulated in the pores in the middle layer of the soil column. The decreased proportion of the <250  $\mu\text{m}$  pores determined by micro-CT scanning (Figure 6), well support this interpretation.

## Figure skipped

**Figure 5** Depth distributions of LAS residues (C<sub>10</sub>-C<sub>13</sub> homologues) in the topsoil (a) and subsoil (b) columns after LAS-enhanced flushing.

For diesel aged soil (Column A1), the removal efficiency of LAS flushing could reach 95% for C<sub>18</sub> n-alkanes in the middle layer of the column. The removal efficiencies of the middle layer of all the *n*-alkanes were highest compare to the top and bottom layers, which may be related to the high residual concentration of the surfactant in the middle layer. There will be a detailed explanation for colloid production and migration part later. For short chain n-alkanes, C<sub>14</sub> and C<sub>16</sub> alkanes have smaller molecular formula and the volatility are relatively stronger (the removal efficiency is not considered C<sub>12</sub> n-alkanes for its stronger volatility), so that, the migration of them by surfactant compatibilization process during flushing are less easily than C<sub>18</sub> in the middle and bottom of the soil column. For the effect of the surfactants on solubilization and mobilization of alkanes decrease with the chain of alkanes increasing, the removal rates of n-alkanes decrease during flushing experiment. The removal efficiency of B1 column was not significant because of the low concentration of alkanes in the non-tillage layer

iscussion

## Conclusions

In the present study, LAS-enhanced flushing experiments were conducted for intact columns of diesel-contaminated farmland purple soil. Results showed that LAS flushing could lead to high colloid discharge and decrease in soil macroporosity particularly the total volume of fine macropores (equivalent pore diameter <250 μm). This phenomenon can be attributed to enhanced clogging of fine macropores by colloids which exhibited higher concentration due to better colloid dispersion by LAS. Feasibility of applying surfactant-enhanced soil flushing technique at contaminated sites should be tested and evaluated at multiple scales from laboratory to field with respect to colloid discharge and soil pore structure.

**6 Effects of LAS-enhanced flushing on transport of colloids and solutes and various soil properties of diesel-contaminated soil after two-year field ageing**

**Figure skipped**

**6.3.2 Effects on depth distributions of LAS and alkanes residues in soil**



16-20	Before flushing	m g kg <sup>-1</sup>	0.35	0.93	1.96	1.43	1.01	0.67	0.39	0.10
	After flushing	m g kg <sup>-1</sup>	0.35	0.35	0.32	0.36	0.21	0.20	0.20	0.06
	Removal rate	%	1.80	62.6	83.7	75.0	79.2	69.7	48.5	45.9
				0	1	9	2	3	5	9
20-24	Before flushing	m g kg <sup>-1</sup>	0.31	0.75	2.41	1.64	1.19	0.84	0.50	0.14
	After flushing	m g kg <sup>-1</sup>	0.26	0.26	0.14	0.21	0.10	0.24	0.21	0.08
	Removal rate	%	21.4	65.2	94.2	87.0	91.6	71.1	58.3	42.6
			8	5	8	5	3	4	7	0

ND means the concentrations of *n*-alkanes are below the detection limits

		Percentage (%)						
		0.00- 0.18	0.18- 0.36	0.36- 0.54	0.54- 0.72	0.72- 0.90	>0.90	
macropores	A1- contaminated	3.27	4.71	5.09	6.58	63.08	17.27	
	A1-flushed	2.55	4.74	5.98	8.47	63.57	14.69	
	B1- contaminated	2.88	4.63	4.73	6.79	64.83	16.14	
	B1-flushed-A	6.51	5.04	3.96	6.53	63.48	14.47	
	throat	A1- contaminated	56.68	13.70	7.30	4.73	1.11	16.48
		A1-flushed	58.59	13.85	6.18	4.47	1.41	15.51
B1- contaminated		60.58	13.01	6.02	7.38	0.78	12.23	
	B1-flushed-A	75.27	6.55	3.27	3.64	0.73	10.55	

## 7 Conclusions

### 7.1 Conclusions

There is a lack of integrated research which can relate the chemical changes in soil and water induced by surfactant-enhanced soil flushing treatment to the changes in soil microstructure, soil water retention characteristics and hydraulic conductivity, surface and interfacial tension, and colloidal properties.

The major portion of n-alkanes of diesel was retained in surface soil layer (0-12cm) and could hardly migrate downwards to greater depths one year after diesel addition.

Long chain n-alkanes can persist in the soil for a long period and migrate downwards to greater depths.

LAS flushing could lead effective removal n-alkanes than that by water flushing.

High colloid discharge in the effluent was observed during LAS flushing and the colloids change to larger sizes.

Colloid transport through macropores in the purple soil may lead to pore plugging particularly the total volume of fine macropores (equivalent pore diameter  $<250 \mu\text{m}$ ).

Feasibility of applying surfactant-enhanced soil flushing technique at contaminated sites should be tested and evaluated at multiple scales from laboratory to field with respect to colloid discharge and soil pore structure.

## References

- American Public Health Association. 1995. Standard methods for the examination of water and wastewater. United Book Press, Baltimore, MD
- Davezza M, Fabbri D, Prevot AB, et al. (2011) Removal of alkylphenols from polluted sites using surfactant-assisted soil washing and photocatalysis. *Environmental Science and Pollution Research* 18(5):783-789 DOI: 10.1007/s11356-010-0427-7
- Dong H (2007) micro-CT imaging and pore network extraction. PhD thesis, Imperial College London, UK. p 213.
- Du Y, Shen C Zhang H et al. (2013) Effects of flow velocity and nonionic surfactant on colloid straining in saturated porous media under unfavorable conditions. *Transport in Porous Media* 98(1):193-208 DOI: 10.1007/s11242-013-0140-3
- Dwarakanath V, Pope G (2000) Surfactant phase behavior with field degreasing solvent. *Environmental science and technology* 34(22): 4842-4848 DOI: 10.1021/es0009121
- Falciglia P.P., Giustra M.G., Vagliasindi F.G.A. (2011) Low-temperature thermal desorption of diesel polluted soil: Influence of temperature and soil texture on contaminant removal kinetics. *Journal of Hazardous Materials* 185(1):392-400 DOI: 10.1016/j.jhazmat.2010.09.046
- Gabr MA, Chen J, Thomas R (2011) Soil clogging during surfactant-enhanced flushing of naphthalene -contaminated sand-kaolinite. *Canadian geotechnical journal* 35(35): 976-985 DOI: 10.1139/cgj-35-6-976
- Garbout A, Munkholm LJ, Hansen SB (2013) Temporal dynamics for soil aggregates determined using X-ray CT scanning. *Geoderma* 204-205(4): 15-22 DOI: 10.1016/j.geoderma.2013.04.004
- Gardner KH, Arias MS (2000) Clay swelling and formation permeability reductions induced by a nonionic surfactant. *Environmental science and technology* 34(1): 160-166 DOI: 10.1021/es990676y
- Guan Z, Huang Y, Wang W (2008) Carboxyl modified multi-walled carbon nanotubes as solid-phase extraction adsorbents combined with high-performance liquid chromatography for analysis of linear alkylbenzene sulfonates. *Analytica Chimica Acta* 627(2):225-231 DOI: 10.1016/j.aca.2008.08.035

Hernández-Espriú A, Sánchez-León E, Martínez-Santos P, et al. (2013) Remediation of a diesel-contaminated soil from a pipeline accidental spill: enhanced biodegradation and soil washing processes using natural gums and surfactants. *Journal of Soils Sediments* 13(1):152-165 DOI: 10.1007/s11368-012-0599-5

Jia LQ, Ou ZQ, Ouyang ZY (2005) Ecological behavior of linear alkylbenzene sulfonate (LAS) in soil-plant systems. *Pedosphere* 15(2):216-224. ISBN: 1002-0160

Khalladi R, Benhabiles O, Bentahar F, Moulai-Mostefa N (2009) Surfactant remediation of diesel fuel polluted soil. *Journal of Hazardous Materials* 164(2-3):1179-1184  
DOI: 10.1016/j.jhazmat.2008.09.024

Laha S, Tansel B, Ussawarujikulchai (2009) A Surfactant–soil interactions during surfactant-amended remediation of contaminated soils by hydrophobic organic compounds: A review. *Journal of Environmental Management* 90(1): 95-100 DOI: 10.1016/j.jenvman.2008.08.006

Lamande M, Wildenschild D, Berisso FE et al. (2013) X-ray CT and laboratory measurements on glacial till subsoil cores: assessment of inherent and compaction-affected soil structure characteristics. *Soil Science* 178(7): 359-368 DOI: 10.1097/SS.0b013e3182a79e1a

Lee CY, Choi MH, Han JI, et al. (2013) A low-foaming and biodegradable surfactant as a soil-flushing agent for diesel-contaminated soil. *Separation Science and Technology* 48(12): 1872-1880 DOI: 10.1080/01496395.2013.779711

Lee M, Kang H, Do W (2005) Application of nonionic surfactant-enhanced in situ flushing to a diesel contaminated site. *Water Research* 39(1): 139-146. DOI: 10.1016/j.watres.2004.09.012

Liu M, Roy D (1995) Surfactant-induced interactions and hydraulic conductivity changes in soil. *Waste Management* 15(7): 463-470 DOI:10.1016/0956-053X(95)00046-3

Lee YC, Woo SG, Choi ES, et al. (2012) Bench-scale ex situ diesel removal process using a biobarrier and surfactant flushing. *Journal of Industrial and Engineering Chemistry* 18(3): 882-887 DOI:10.1016/j.jiec.2012.01.020

Mao XH, Jiang R, Xiao W, et al. (2015) Use of surfactants for the remediation of contaminated soils: A review. *Journal of Hazardous Materials* 285:419-435  
DOI: 10.1016/j.jhazmat.2014.12.009

Martinez F, Martin M, Caniego F et al. (2010) Multifractal analysis of discretized X-ray CT

imagesfor the characterization of soil macropore structures. *Geoderma* 156(1-2): 32-42 DOI: 10.1016/j.geoderma.2010.01.004

Matthew A, Cowell. Kibbey TC, Zimmerman JB, et al. (2000) Partitioning of Ethoxylated Nonionic Surfactants in Water/NAPL Systems: Effects of Surfactant and NAPL Properties. *Environmental science and technology* 34(8):1583-1588 DOI: 10.1021/es9908826

Svab M, Kubal M, Müllerova M, Raschman R (2009) Soil flushing by surfactant solution: pilot-scale demonstration of complete technology. *Journal of Hazardous Materials* 163(1): 410-417 DOI: 10.1016/j.jhazmat.2008.06.116

Park SK, Bielefeldt AR (2005) Non-ionic surfactant flushing of pentachlorophenol from NAPL-contaminated soil. *Water Research* 39(7):1388-1396 DOI: 10.1016/j.watres.2005.01.009

Pasha AY, Hu LM, Meegoda JA, et al. (2012) Centrifuge Modeling of In situ Surfactant Enhanced Flushing of Diesel Contaminated Soil. *Geotechnical Testing Journal* 34(6) 1-11 DOI: 10.1520/GTJ103695

Pennell KD, Abriola LM.,Weber WJ (1993) Surfactant-enhanced solubilization of residual dodecane in soil columns 1.Experimental investigation. *Environmental Science and Technology* 27(12): 2332-2340 DOI: 10.1021/es00048a005

Renshaw CE, Zynda GD, Fountain JC (1997) Permeability reductions induced by sorption of surfactant. *Water Resources Research* 33(3):371-378 DOI: 10.1029/96WR03299

Rosas JM, Vicente F, Santos A, et al. (2011) Enhancing p-cresol extraction from soil, *Chemosphere* 84(2):260-264 DOI: 10.1016/j.chemosphere.2011.03.071

Roy D, Kongara S, Valsaraj KT (1995) Application of surfactant solutions and colloidal gas apron suspensions in flushing naphthalene from a contaminated soil matrix. *Journal of Hazardous Materials* 42(3): 247-263 DOI: 10.1016/0304-3894(95)00018-P

Tang XY, Zhu B, Katou H (2012) A review of rapid transport of pesticides from sloping farmland to surface waters: Processes and mitigation strategies. *Journal of Environmental Sciences* 24(3) 351-361 DOI: 10.1016/S1001-0742(11)60753-5

Trellu C, Mousset E, Pechaud Y, et al. (2015) Removal of hydrophobic organic pollutants from soil washing/flushing solutions: A critical review. *Journal of Hazardous Materials* 306:149-174 DOI: 10.1016/j.jhazmat.2015.12.008

Urum K, Grigson S, Pekdemir T et al. (2006) A comparison of the efficiency of different

surfactants for removal of crude oil from contaminated soil. *Chemosphere* 62(9): 1403-1410  
DOI: 10.1016/j.chemosphere.2005.05.016

Vishnyakov A, Lee M.T., Neimark A.V. (2013) Prediction of the critical micelle concentration of nonionic surfactants by dissipative particle dynamics simulations, *Journal of Physical Chemistry Letters* 4(4): 797-802 DOI: 10.1021/jz400066k

Wang J, Guo L, Bai Z et al. (2016) Using computed tomography (CT) images and multi-fractal theory to quantify the pore distribution of reconstructed soils during ecological restoration in opencast coal-mine. *Ecological Engineering* 92:148-157  
DOI: 10.1016/j.ecoleng.2016.03.029

Zhang W, Tang XY, Weisbrod, N, et al. (2015) A coupled field study of subsurface fracture flow and colloid transport. *Journal of Hydrology* 524:476-488 DOI: 10.1016/j.jhydrol.2015.03.001

Zhang W, Tang XY, Xian QS, et al. (2016) A field study of colloid transport in surface and subsurface flows. *Journal of Hydrology* 542:101-114 DOI:10.1016/j.jhydrol.2016.08.056

M. Arias-Estévez, E. López-Periago, E. Martínez-Carballo, J. Simal-Gándara, J.-C. Mejuto, L. García-Río, The mobility and degradation of pesticides in soils and the pollution of groundwater resources, *Agric. Ecosyst. Environ.* 123 (2008) 247–260.

P.C. Zhang, J.L. Krumhansl, P.V. Brady, Introduction to properties, sources and characteristics of soil radionuclides, in: P.C. Zhang, P.V. Brady (Eds.), *Geochemistry of Soil Radionuclides*, Soil Science Society of America, 2002, pp. 1–20.

Ettore Trulli ,Cristiana Morosini ,Elena C. Rada andVincenzo Torretta Remediation in Situ of Hydrocarbons by Combined Treatment in a Contaminated Alluvial Soil due to an Accidental Spill of LNAPL *Sustainability* 2016, 8(11), 1086; doi:10.3390/su8111086

Amechi S. Nwankwegua, Michael U. Orjia, Chukwudi O. Onwosib Studies on organic and inorganic biostimulants in bioremediation of diesel-contaminated arable soil. *Chemosphere* Volume 162, November 2016, Pages 148–156

Leticia A. Bernardez,, René Therrien, René Lefebvre, Richard Martel . Simulating the injection of micellar solutions to recover diesel in a sand column. *Journal of Contaminant Hydrology* 103 (20 09) 99 – 108

U.S. EPA, 2003, Treatment technologies for site cleanup: annual status report, 11th ed., EPA 542-R-03-009.

USEPA, 2006, "In Situ Treatment Technologies for Contaminated Soil,"EPA 542/F-06/013.

Lee, L. S., Zhai, X., and Lee J., 2007, "Guidance Document for In-situ Soil Flushing Remediation," Transportation Research Program SPR-2335, FHWA/IN/JTRP-2006/28.

J.C. Fountain, R.C. Starr, T. Middleton, M. Beikirch, C. Taylor, D. Hodge, A controlled field test of surfactant-enhanced aquifer remediation, *Groundwater* 34 (1996) 910–916.

D. Lestan, C.-L. Luo, X.-D. Li, The use of chelating agents in the remediation of metal-contaminated soils: a review, *Environ. Pollut.* 153 (2008) 3–13.

G. Dermont, M. Bergeron, G. Mercier, M. Richer-Lafleche, Soil washing for metal removal: a review of physical/chemical technologies and field applications, *J. Hazard. Mater.* 152 (2008) 1–31.

L.S. Lee, X. Zhai, J. Lee, INDOT Guidance Document for In-Situ Soil Flushing, Indiana Department of Transportation and Purdue University, West Lafayette, Indiana, 2007,

C.N. Mulligan, R.N. Yong, B.F. Gibbs, Surfactant-enhanced remediation of contaminated soil: a review, *Eng. Geol.* 60 (2001) 371–380.

U.S. EPA, 2003, Treatment technologies for site cleanup: annual status report, 11th ed., EPA 542-R-03-009.

USEPA, 2006, "In Situ Treatment Technologies for Contaminated Soil,"EPA 542/F-06/013.

Lee, L. S., Zhai, X., and Lee J., 2007, "Guidance Document for In-situ Soil Flushing Remediation," Transportation Research Program SPR-2335, FHWA/IN/JTRP-2006/28.

A. Vishnyakov, M.T. Lee, A.V. Neimark, Prediction of the critical micelle concentration of nonionic surfactants by dissipative particle dynamics simulations, *J. Phys. Chem. Lett.* 4 (2013) 797–802.

B.-K. Kim, K. Baek, S.-H. Ko, J.-W. Yang, Research and field experiences on electrokinetic remediation in South Korea, *Sep. Purif. Technol.* 79 (2011) 116–123

Bettahar, M., Schafer, G., and Baviere, M., 1999, "An Optimized Surfactant Formulation for the Remediation of Diesel Oil Polluted Sandy Aquifers," *Environ. Sci. Technol.* , Vol. 33, No. 8, pp. 1269–1273.

Sabatini, D. A., Harwell, J. H., and Knox, R.C., 1999, "Surfactant Selection Criteria for Enhanced Subsurface Remediation," *ACS Symp. Ser.*, Vol. 725, Chapter 2, pp. 8–23.

F. Fernandez Perez, M.D. Luque de Castro, Micelles training for improvement of continuous subcritical water extraction of polycyclic aromatic hydrocarbons in soil prior to high performance liquid chromatography fluorescence detection, *J. Chromatogr. A* 902 (2000) 357–367.

M.C. Chang, C.R. Huang, H.Y. Shu, Effects of surfactants on extraction of phenanthrene in spiked sand, *Chemosphere* 41 (2000) 1295–1300.

D.F. Lowe, C.L. Oubre, C.H. Ward, *Surfactant and Cosolvents for NAPL Remediation*, Lewis, New York, 1999.

S. Fiorenza, C.A. Miller, C.L. Oubre, C.H. Ward, *NAPL Removal: Surfactants, Foams, and Microemulsions*, Lewis, Florida, 2000.

A. Lohi, M. Alvarez-Cuenca, G. Anania, S.R. Upreti, L. Wan, Biodegradation of diesel fuel-contaminated wastewater using a three-phase fluidized bed reactor, *J. Hazard. Mater.* 154 (2008) 105-111.

U.S. EPA, *In-situ treatment technologies for contaminated soil*, Office of Solid Waste and Emergency Response, EPA-542-F-06-013,2006.

M. Lee, J. Kim, I. Kim, In-situ biosurfactant flushing, coupled with a highly pressurized air injection, to remediate the bunker oil contaminated site, *Geosci. J.*15 (2011) 313–321

Liu, M.W., Roy, D. Surfactant-induced interactions and hydraulic conductivity changes in soil. *Waste Management*, 1995, 15(7): 463-470.

Tumeo, M.A. A survey of the causes of surfactant-induced changes in hydraulic conductivity. *Ground Water Monitoring and Remediation*, 1997, 17(4): 138-144.